DANMARKS OG GRØNLANDS GEOLOGISKE UNDERSØGELSE RAPPORT 2008/8

Gold favourability in the Nuuk region, southern West Greenland: results from fieldwork follow-up on multivariate statistical analysis

Mineral resource assessment of the Archaean Craton (66° to 63°30'N) SW Greenland Contribution no. 9

Bo Møller Stensgaard

GEOLOGICAL SURVEY OF DENMARK AND GREENLAND
MINISTRY OF CLIMATE AND ENERGY

GEUS

DANMARKS OG GRØNLANDS GEOLOGISKE UNDERSØGELSE RAPPORT 2008/8

Gold favourability in the Nuuk region, southern West Greenland: results from fieldwork follow-up on multivariate statistical analysis

Mineral resource assessment of the Archaean Craton (66° to 63°30'N) SW Greenland Contribution no. 9

Bo Møller Stensgaard

GEOLOGICAL SURVEY OF DENMARK AND GREENLAND
MINISTRY OF CLIMATE AND ENERGY

GEUS

Contents

Abstract

This report documents the results of the fieldwork carried out in 2006 under the project 'Multiparameter Geologcial Modelling'. The fieldwork was carried out in selected areas that in earlier phases of the project have been outlined as being favourable for gold. The objectives of the fieldwork were to characterise the selected areas, investigate possible sources for the predicted favourability of the individual area and examine the gold potential.

One of the visited outlined favourable areas, located in the inner part of Fiskefjord, is of special interest. This is one of the largest areas outside the central Nuuk region outlined as favourable for gold and lies outside the presently known gold bearing supracrustal belts in the Godthåbsfjord area. However, no exploration for gold has been undertaken in the outlined area. A large lithological diversity ranging from large ultramafic dunites and pyroxenites bodies, norite bodies, amphibolites of magmatic and possible also non-magmatic origin, metasediments, gneisses (TTGs), later granites, pegmatites and lamprophyric dykes were found in the area. A pervasive epidotisation was encountered at several localities in the inner Fiskefjord, which is taken as evidence for a pronounced hydrothermal activity along the marked Fiskefjord fault. Sulphide mineralisation was discovered in several places; both as semi-massive and disseminated iron-sulphides in amphibolites and as disseminated iron-sulphides in quartz-rich parts of amphibolite (possible silicified) and quartz veins. The rock units in the area displays in several cases elevated gold content in the order of >10 ppb Au to 377 ppb Au.

In general, for all visited favourable areas were it confirmed, that all predicted most favourable areas (top 0.5% to 2.5–5%) were located within or adjacent to supracrustal rock units, which to variable degree resembles those with known gold mineralisation in the Nuuk region. The areas were furthermore found to contain many interesting features for gold mineralisation processes such as a larger diversity in lithologies and various indications of hydrothermal activities. Characteristic data signatures for gold occurrences in the Nuuk region were also found to be present in many of the visited favourable area; verifying the statistical extraction of the signatures and the potential for gold.

Regional geology and known gold showings

Stensgaard *et al.* (2006b) presented maps for the Nuuk region with a classification of the area in terms of favourability for gold mineralisation. The classification is based on a multivariate statistical analysis of known gold showings in relation to geochemical and geophysical data. The multivariate statistical analysis identified three groups of mineral occurrences with distinct differences in geochemical and geophysical signature (Stensgaard *et al.* 2006b). The defined data signatures of the three groups of gold showings together with a short description of the methods used for identifying the groups and extraction of the signatures, are summaries in Appendix A (Table 21). The three groups named after the primary location of the mineralisations are the Storø, Bjørneøen and Isua gold groups. The locations of the showings are marked on the simplified geological maps in Figure 1.

This report is based on a field follow-up of selected areas that from the multivariate statistical analysis were predicted as the most favourable areas for gold mineralisation similar to those defining the three groups. Geological descriptions and results from geochemical analysis of collected rock and stream sediments data are presented and discussed.

The Nuuk region (Fig. 1) represents a deeply eroded complex amalgamation of six Eo- to Meso-Neoarchaean crustal terranes (Friend & Nutman 2005). Summaries by their age starting with the oldest the terranes are the Isukasia and Færingehaven terranes (*c.* 3850 to 3300 Ma), the Akia terrane (*c.* 3200 to 2975 Ma), the Kapisillik (*c.* 3075 to 2960 Ma), the Tasiusarsuaq terrane (*c.* 3000 to 2800 Ma), and the Tre Brødre terrane (*c.* 2826 to 2750 Ma). The terranes were amalgamated in the period from 2950 Ma to 2700 Ma and are bounded by tectonic features such as faults and shear zones. The terranes are dominated by quartzo-feldspathic orthogneiss, but with a significant proportion of supracrustal-granite belts, and some contain greenstones. The belts represent remnants of Archaean geological environments, mainly magmatic, island arc, ocean floor and/or accretional environments. The most common rock type is amphibolite of tholeiitic to komatiitic composition, but andesitic compositions have also been recognised in the region. Metasedimentary rocks are mostly garnet-mica schist. Bodies of mafic to ultramafic rocks are common within the supracrustal belts. Primary geological environments dominated by magmatism (ocean-floor intrusives; e.g. the NordlandetFiskefjord area), island-arc settings (e.g. the Qussuk area) and accretionary settings (e.g. Storø) exists in the region. The Nuuk region also records a complex history of high-grade metamorphism and deformation, which affected different part of the region at different time, from 3.8–2.5 Ga. The regional assemblage of the terranes was post-dated by the emplacement (*c.* 2530 Ma) of the Qôrqut sheeted granite complex. Post-Archaean event include the intusion of Proterozoic dolerite dykes (2400–2200 Ma) and regional-scale faulting, e.g. the NE–SW-trending Kobbefjord, Fiskefjord and Ataneq fault.

New aspects of the regional geology and the supracrustal belts have recently been addressed in several reports and papers, e.g. Appel *et al.* 2005; Friend & Nutman 2005; Garde *et al.* 2007; Hollis 2005; Hollis *et al.* 2004; Hollis *et al.* 2006a, b; Knudsen *et al.* 2007; Persson, 2007; Nielsen *et al.* 2004; Stensgaard *et al.* 2006a, b.

Gold mineralisations have been located at a number of sites within almost all larger supracrustal belts. Elevated gold concentrations are encountered in supracrustal rocks exhibiting signs of hydrothermal alteration such as quartz veining, silicification, seritization, garnetisation, leaching and carbonatisation. Genetic models for the gold mineralisations within the region are being debated and are still uncertain. However, it seems that both orogenic (mesothermal lode gold) and epithermal high-sulphidation gold systems and/or stratabound (high-suphidation) gold systems may be present. The gold mineralisations and their setting in the Nuuk region have been addressed in various works; e.g. Appel *et al.* 2000; Appel *et al.* 2005; Garde 2007; Juul-Pedersen *et al.* 2007; Pasi *et al.* 2006.

In this work, the locations of recorded gold content in collected rock samples with values above 1 ppm Au have been used to identify 52 gold showings (in the statistical treatment the Nuuk area is divided into a regular grid with cell sizes of 200 m × 200 m, and a showing is here defined as grid cell in which one or more *in situ* rock samples have 1 ppm Au or more). The showings at Qussuk, Aappalaartoq and Qingaaq are currently targets from commercial exploration by the company NunaMinerals A/S (lincense number 2002/07).

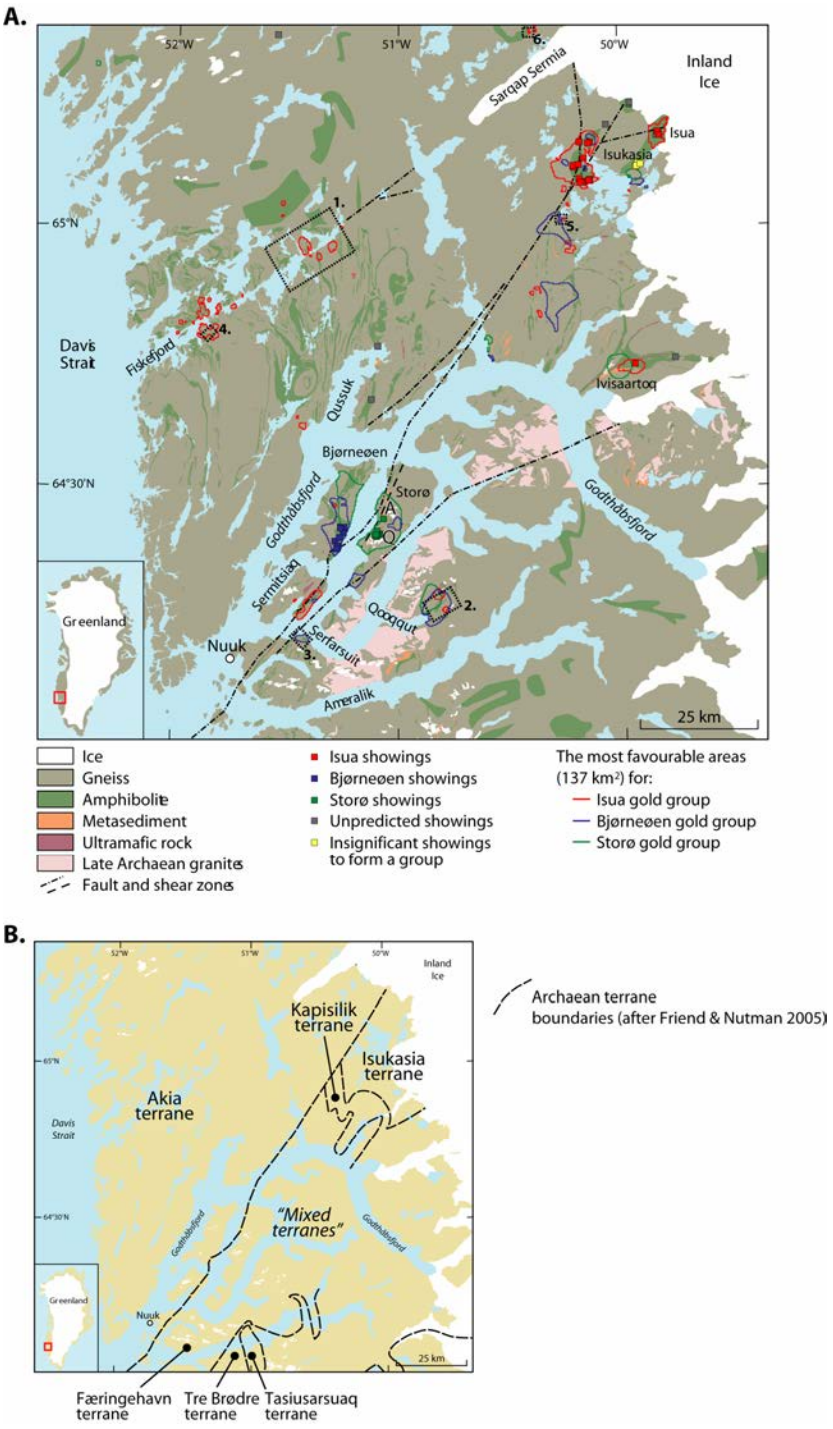

Figure 1. ***A:*** *Simplified geological map of the Nuuk region with outline of the predicted most favourable (137 km^2) areas for the three gold groups defined in Stensgaard et al. (2006b). The locations of the gold showings of the groups are indicated with colour-filled squares. The outline of the rock units are from digital versions of the 1:100 000 and 1:500 000 scale geological maps (Chadwick & Coe 1988; Escher & Pulvertaft 1995; Garde 1989; McGregor 1983). The gold showings at central Storø comprise the Aappalaartoq and Qingaaq gold prospects (A and Q respectively on the map), which are investigated by the exploration company NunaMinerals A/S. The numbered rectangles indicates the areas visited during the fieldwork. These numbers are also used in the headings for the sections of this report dealing with the different areas.* ***B:*** *Simplified overview of the different Archaean terranes in the Nuuk region.*

Favourability for gold in the Nuuk region – field follow-up 2006

The fieldwork conducted in 2006 as part of the GEUS and BMP financed Multiparameter Geological Modelling 2006/07 project (Stensgaard *et al.* 2006b, a) had three principal objectives:

1. Test the favourability predictions and provide information on possible sources to the established characteristic data signatures in areas predicted as favourable for gold showings (Stensgaard *et al.* 2006b).
2. Sample representative lithologies and mineral occurrences in order to evaluate their geochemical signature, and collect new additional stream sediments samples in the visited areas.
3. Examine the primary depositional environments in order to gain more information on their characteristics.

The fieldwork was carried out by Bo Møller Stensgaard (Project Research Scientist, GEUS) and field-assistant Mie Munck Frandsson (stud. scient., University of Copenhagen) in the period July 10 to August 14, 2006. The work was conducted by foot from four camps and from one location supported by helicopter lift to and from the location, and one reconnaissance by helicopter. A zodiac was used for local transport from two coastal camps. The camp locations and reconnaissance stops are given in Table 1. The work done from Camp02 is not covered by this report, but is addressed in Garde (2007).

Table 1. *Locations of camp and reconnaissance stops during fieldwork in 2006.*

Camp/ stops	Area	Period	Longitude	Latitude	Notes
Camp01	Inner Fiskefjord	12/7 – 27/7	-51.40269	64.96749	Transportation: Zodiac and field traverse by foot. Helicopter lift to and from position north of camp. Visit by Lars Lund Sørensen and Annette Clausen from Bureau of Mineral and Petroleum.
Camp02	Qussuk	27/7 – 2/8	-51.08398	64.72353	27/7 – 2/8: Joint camp together with Adam A. Garde (GEUS) and Thomas Rintza Hansen (stud. scient., University of Copenhagen). 30/7–1/8: Joint camp also together with Henrik Stendal, Anders Schersten, Dirk Frei, (all GEUS) and Jens Konnerup Madsen (University of Copenhagen). Transportation: Zodiac and field traverse by foot. Helicopter reconnaissance 2/8 together with Adam A Garde and Thomas Rintza Hansen.
Camp03	Qooqqut lake	2/8 – 7/8	-50.759740	64.29761	Transportation: field traverses by foot.
Camp04	Serfarsuit	7/8 – 11/8	-51.40584	64.19765	Transportation: field traverses by foot.
Stop A	Outer Fiskefjord	2/8	-51.81336	64.80803	c. 1½ hour stop
Stop B	SW of Isua	2/8	-50.31387	65.02114	c. 1½ hour stop
Stop C	N of Sarqap Sermia Glacier	2/8	-50.45044	65.35221	c. 1 hour stop

Inner Fiskefjord (area 1)

The inner Fiskefjord comprising the areas of Suversoq, Ulamertoq, Kuulik and Alanngortooq is part of the Archaean Akia terrane and is dominated by two groups of quartzofeldspathic orthogneiss with ages of *c.* 3200 and 3000 Ma, several supracrustal associations, ultramafic rock bodies and granitic-pegmatitic sheets (Garde 1997). The accretion and evolution of especially the gneiss have been studied in detail by Garde (1997). A map with a landsat image of the area and the visited localities is given in Figure 2.

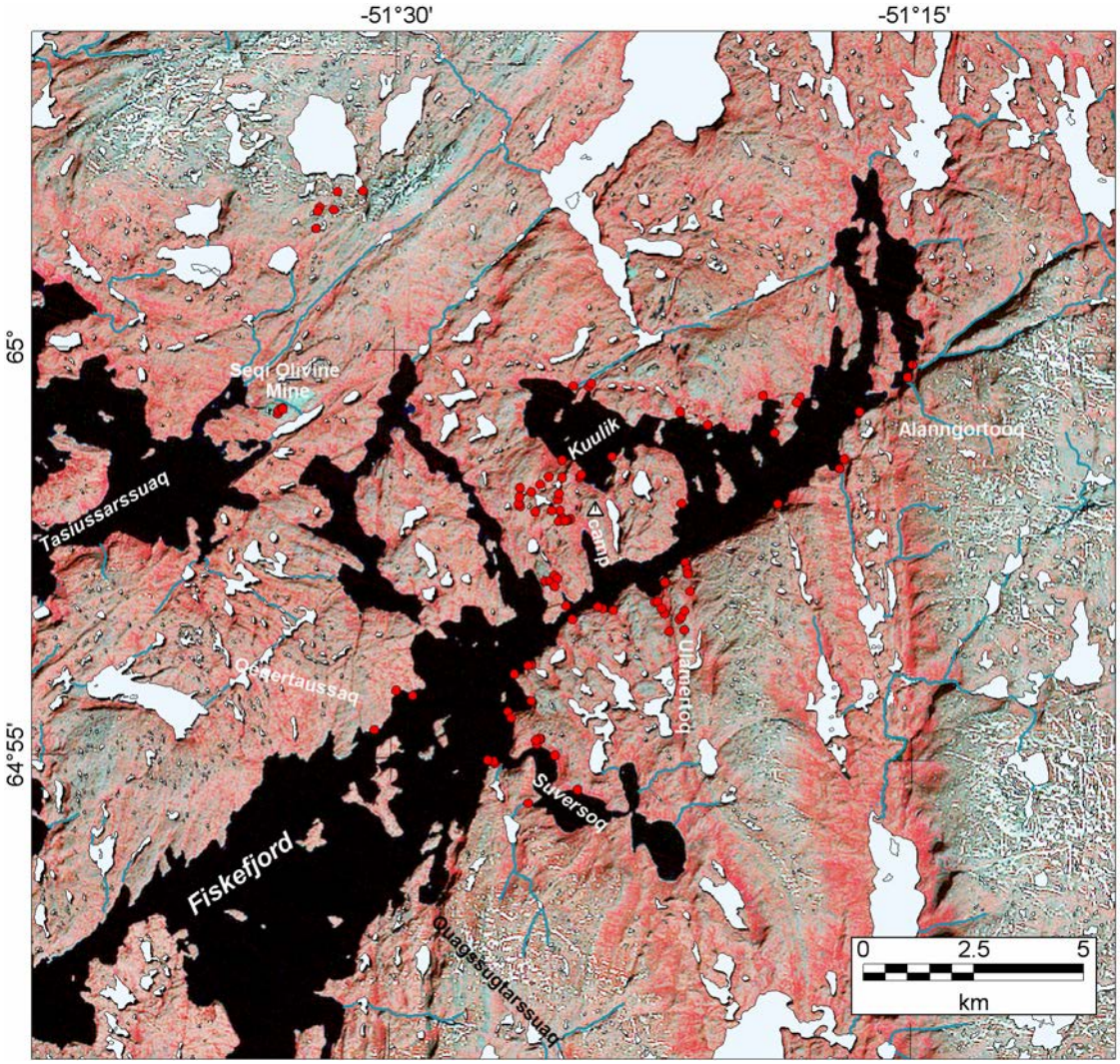

Figure 2. *Landsat image of the inner Fiskefjord area. Visited localities are indicated by red circles and the camp position with a white triangle. The underlying image is a subset of a Landsat image mosaic of entire West Greenland. Areas with vegetation appear red, whereas grey colours indicate barren rock surfaces. Colour composite TM bands 4 (red), 3 (green) and 2(blue) have been used to control the intensities of the red, green and blue colour in the image. The image is enhanced by gaussian stretching filtering.*

Characteristic signatures of the most favourable areas

The areas outlined as most favourable in the inner Fiskefjord, associated with the group of Isua gold showings and the data sets found to be characteristic for this group (Stensgaard *et al.* 2006b), are shown in Figure 3. The mean data values and standard deviation of these gridded data sets in the predicted top 2.5% most favourable areas are given in Figure 4 and Table 2. As seen from in Figure 4, the most pronounced differences between the signatures of the favourable areas and the background signature of the entire study area are lower contents of La, Na_2O and a higher content of MgO, Fe_2O_3, Ni+Cr and MgO/Ni in stream sediment geochemistry.

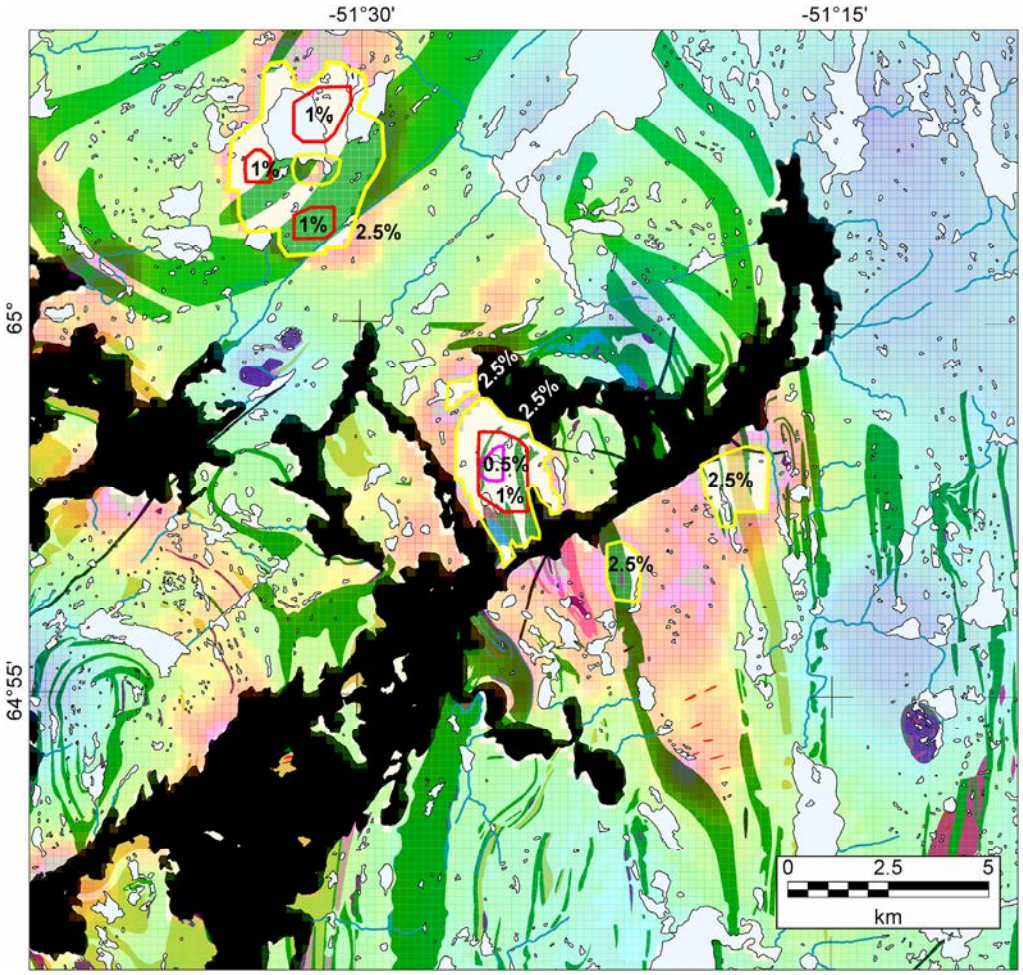

Figure 3. *Transparent gold potential map superimposed on the mapped geology. The potential map is based on the 19 showings of the Isua group (Stensgaard et al. 2006b), and the fine fraction stream sediment geochemistry of Au, Cs, La, MgO, Fe_2O_3, Na_2O, Ni+Cr and Mg/Ni, the vertical gradient of the total magnetic intensity field (VG-TMI), the amplitude of the horizontal gradient of the total magnetic intensity field (Ampl-HG-TMI, and the aeroradiometric eU/Th. These data sets are all found to be characteristic for the Isua group. The top 2.5% most favourable area is shown in transparent white and outlined with yellow polygons. The four largest areas are labelled A–D. The mean values and associated standard deviation of the characteristic data sets for these four areas are given in Table 2 and Figure 4. The top 0.5% and 1% most favourable areas are outlined with magenta and red polygons respectively. See Figure 5 for the geological legend.*

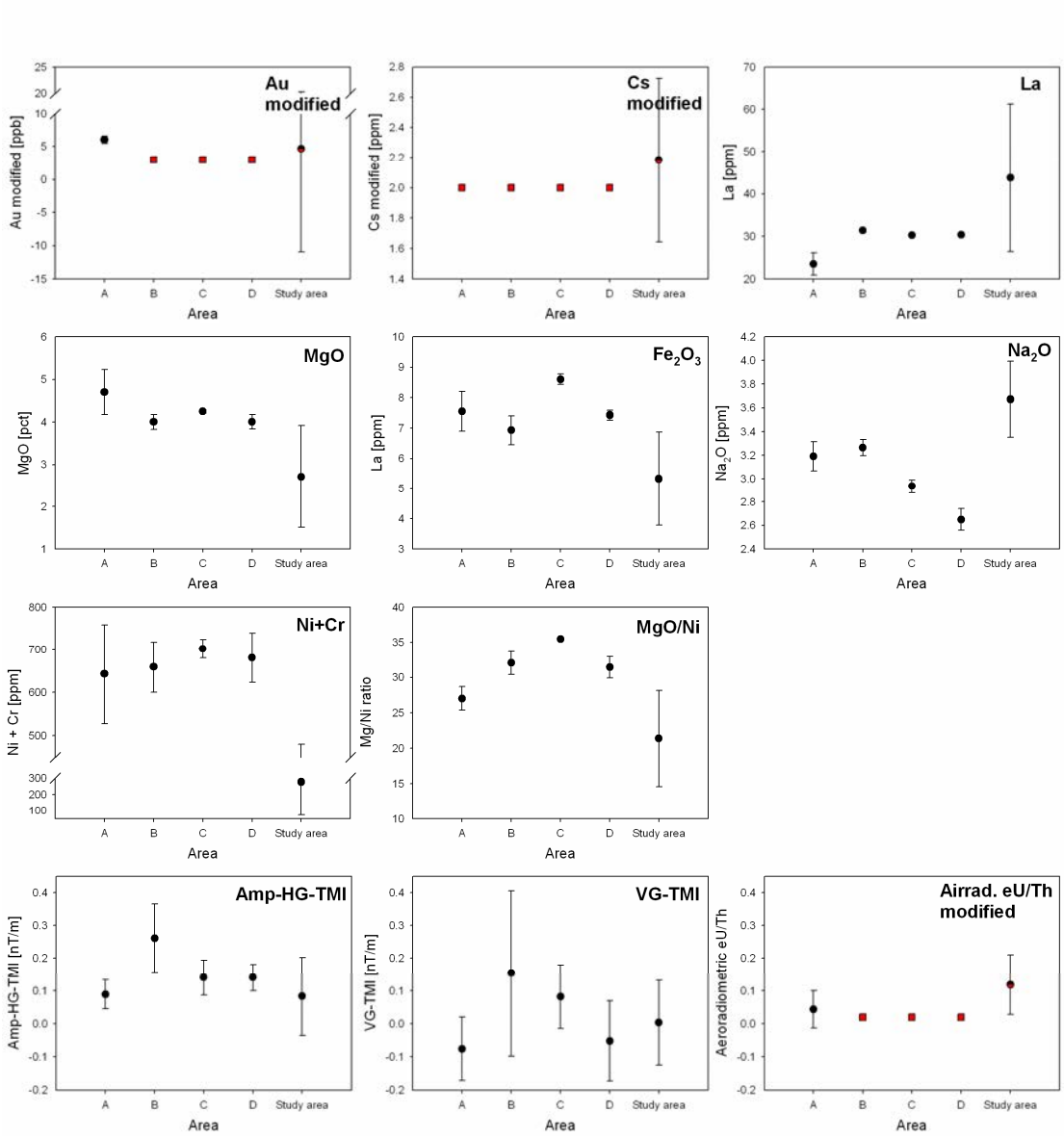

Figure 4. *Plot of the mean values and associated standard deviation extracted from different data grids for the four largest areas belonging to the top 2.5% most favourable area (see Fig. 3) and for the entire study area. The values are also given in Table 2. As discussed in Nielsen et al. (2004), some areas (pixels) for some elements (e.g., As, Au, Cs and Sb) in the grid for the geochemical data have contents below the analytical detection limit (d.l.).This can both be due to the originally obtained geochemical values for the samples and to the gridding of the data. In such cases, grid values (pixels) below d.l. have been set to the value of the d.l. for the particular element. For the aeroradiometric data is a blanking distance of 5000 m to nearest flight line used; areas with pixels outside the blanking distance have been given values identical to the mean of the data variation. Red filled squares for geochemical data indicate that the values of the mean and standard deviation reflect d.l. for geochemical data and the mean of the entire region for aeroradiometric data. Half-red filled circles for the entire study area indicate that the mean and standard deviation are for a modified data set. However, this will only have a minor effect on the statistics for the entire study area as only a smaller part of the entire study area contains modified pixels. Black filled circles imply no modification of the data set.*

Most of the top 2.5% most favourable area are characterised by modified grid pixel values for the Au and Cs content in stream sediment geochemistry; the pixels of these areas have been set to the analytical detection limit (see Fig. 4). Only favourable area A contains pixels without any modifications in the gridded Au stream sediment geochemistry. This area has slightly higher mean Au content (*c.* 6 ppb) compared to the entire study area. There is a tendency towards slightly more positive and negative values for the vertical gradient and the amplitude of the horizontal gradients of the total magnetic field intensity; although not very pronounced. No general trend for the favourable areas can be observed in the areoradiometric eU/Th values as only area A contains pixels without any modifications in the gridded aeroradiometric data (see Fig. 4); the mean values of this area differs from the eU/Th of the entire study area by being slightly lower.

Table 2. *Extracted mean data values and standard deviation of the gridded data found to be characteristic for the Isua group of gold showings (Stensgaard et al. 2006b). VG-TMI and Amp-HG-TMI denotes the vertical gradient and amplitude of the horizontal gradient of the total magnetic intensity field respectively. The extracted values are for the top 2.5% most favourable areas (see Fig.3) in the inner Fiskefjord.*

Area	Mean Au modi. [ppb]	StdDev. mean Au modi.	Mean Cs modi [ppm]	StdDev. mean Cs modi.	Mean La [ppm]	StdDev. La	Mean MgO [pct.]	StdDev. MgO
A	6.06	0.59	2.00	0.00	23.49	2.59	4.70	0.53
B	3.00	0.00	2.00	0.00	31.36	0.42	4.00	0.18
C	3.00	0.00	2.00	0.00	30.25	0.08	4.25	0.04
D	3.00	0.00	2.00	0.00	30.31	0.30	4.00	0.17
Entire study area	4.67	15.60	2.18	0.54	43.80	17.42	2.72	1.21

Area	Mean Fe_2O_3 [pct.]	StdDev. Fe_2O_3	Mean Na_2O [pct.]	StdDev. Na_2O	Mean Ni+Cr [ppm]	StdDev. Ni+Cr	Mean Ni/Mg [ratio]	StdDev. Ni/Mg
A	7.56	0.65	3.19	0.12	642.80	115.57	26.99	1.65
B	6.93	0.47	3.26	0.07	659.37	58.64	32.03	1.63
C	8.60	0.17	2.93	0.05	702.12	21.79	35.44	0.13
D	7.43	0.16	2.65	0.09	681.07	57.62	31.42	1.49
Entire study area	5.33	1.54	3.67	0.32	276.17	204.03	21.38	6.77

Area	Mean VG-TMI [nT/m]	StdDev. VG-TMI [nT/m]	Mean AmpHG-TMI [nT/m]	StdDev. AmpHG-TMI [nT/m]	Mean airrad. eU/Th [ratio]	StdDev. airrad eU/Th
A	-0.08	0.10	0.09	0.04	0.04	0.06
B	0.15	0.25	0.26	0.10	0.02	0.00
C	0.08	0.10	0.14	0.05	0.02	0.00
D	-0.05	0.12	0.14	0.04	0.02	0.00
Entire study area	0.00	0.13	0.08	0.12	0.11	0.09

Geological observations

Many smaller belts of supracrustal rocks (up to *c.* 1.5 km wide), mainly amphibolite, are found in the inner part of Fiskefjord (Fig. 5). The orthogneiss in the entire Fiskefjord region has been investigated in details by Garde (1997). The supracrustal rocks are intercalated with grey gneiss retrogressed to amphibolite facies with ages from *c.* 3221±13 Ma to 3110±40 Ma (Garde 1997). Garde obtained a compositional range of the gneisses from granodioritic–quartz dioritic to tonalitic–trondhjemitic. Based on the analytical work, a distinct group of dioritic gneiss, the *c.* 3050 Ma Qeqertaussaq diorite, was found to be characteristic for the inner Fiskefjord (Garde 1997).

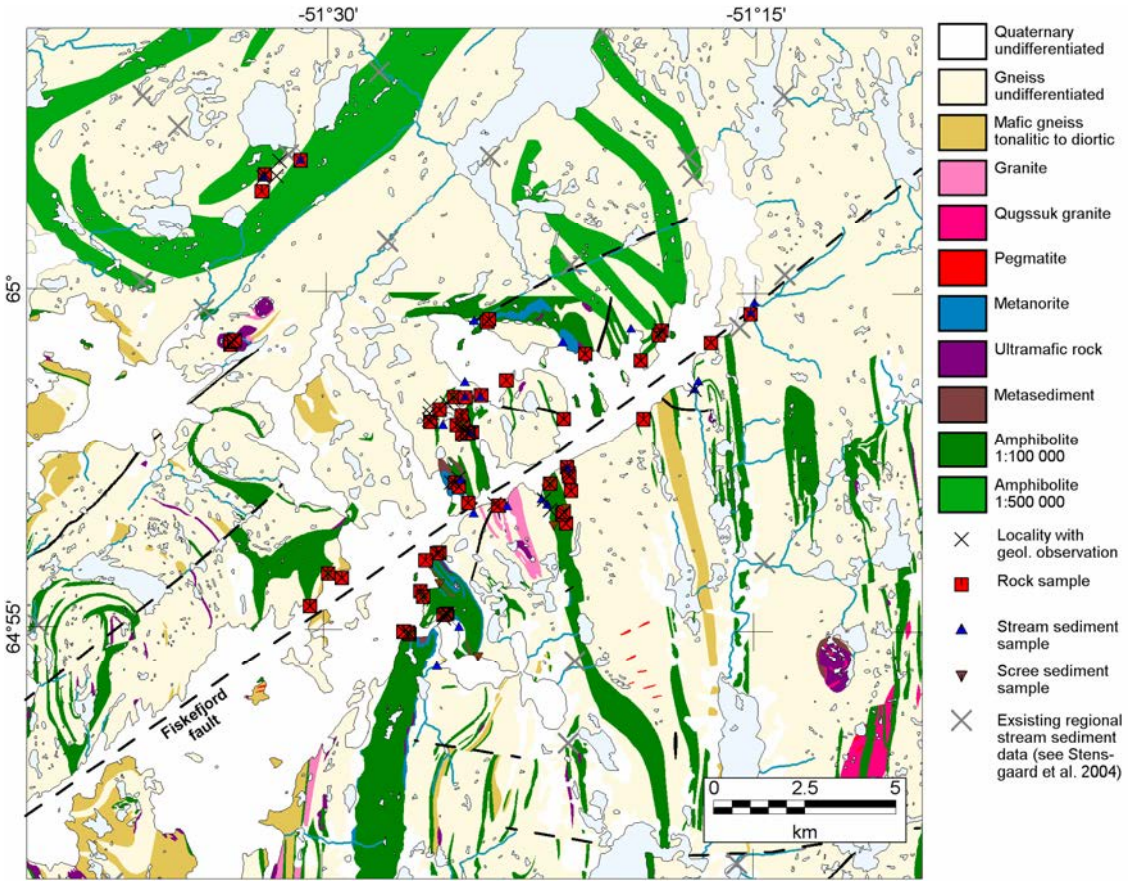

Figure 5. *Geological maps of the inner Fiskefjord area with position of visited localities and samples. Major fault zones, with the Fiskefjord Fault as the most striking, are also indicated. South of latitude 65° are mapped units from the digital version of the Fiskefjord geological map sheet in scale 1:100 000 used (Garde 1989), northwards are shown mapped units based on a georeferenced raster image of the Frederikshåb Isblink – Søndre Strømfjord map sheet in scale 1:500 000 (Allaart 1982).*

Table 3. *Overview of localities and samples from the inner Fiskefjord.*

Locality	Rock sample no.	Locality	Rock sample no.	Locality	Stream sediment sample no.
2006bms001	482001	2006bms056	482037	2006bms005	507801
2006bms003	482002	2006bms056	482038	2006bms009	507803
2006bms006	482003	2006bms057	482039	2006bms016	507805
2006bms007	482004	2006bms057	482040	2006bms025	507808
2006bms010	482005	2006bms058	482041	2006bms031	507812
2006bms011	482006	2006bms060	482042	2006bms033	507814
2006bms012	482007	2006bms061	482043	2006bms038	507817
2006bms014	482008	2006bms064	482044	2006bms041	507816
2006bms015	482009	2006bms067	482045	2006bms044	507818
2006bms017	482010	2006bms069	482046	2006bms059	507820
2006bms019	482010	2006bms069	482047	2006bms062	507821
2006bms020	482012	2006bms070	482048	2006bms063	507822
2006bms022	482013	2006bms074	482049	2006bms065	507823
2006bms025	482014	2006bms074	482050	2006bms066	507824
2006bms026	482015	2006bms076	482051	2006bms068	507825
2006bms028	482016	2006bms077	482052	2006bms072	507827
2006bms029	482017	2006bms078	482053	2006bms075	507830
2006bms030	482018	2006bms080	482054	2006bms079	507832
2006bms034	482019	2006bms082	482055	2006bms081	507833
2006bms035	482020	2006bms083	482056	2006bms084	507834
2006bms036	482021	2006bms087	482057	2006bms085	507835
2006bms038	482022	2006bms088	482058	2006bms086	507850
2006bms040	482023	2006bms089	482059	**Locality**	**Scree sediment sample no.**
2006bms042	482024	2006bms090	482060	2006bms013	507804
2006bms042	482025	2006bms091	482061	2006bms019	507806
2006bms043	482026	2006bms092	482062	2006bms022	507807
2006bms045	482027	2006bms093	482063	2006bms026	507809
2006bms045	482028	2006bms094	482064	2006bms028	507810
2006bms045	482029	2006bms095	482065	2006bms030	507811
2006bms049	482030			2006bms032	507813
2006bms050	482031			2006bms034	507819
2006bms051	482032			2006bms056	507819
2006bms052	482033			2006bms071	507826
2006bms054	482034			2006bms073	507828
2006bms055	482035			2006bms077	507831
2006bms055	482036			2006bms096	507836

The dominating amphibolites in the visited areas form a uniform mafic light- to dark-grey homogeneous, fine- to medium-grained, in some cases thick banded, rock type with hornblende (amphiboles), plagioclase, quartz, and biotite (dark mica). Platy appearances of the amphibolite, probably due to deformation, are encountered in some areas. This type of amphibolite is similar to the homogeneous amphibolite described by Garde (1997). The homogeneous amphibolites are found as rather thick sequences (10–100's m wide) intercalated in orthogneisses and intruded by pegmatites. Thinner sequences of more heterogeneous mafic grey amphibolite, also described by Garde (1997), are also encountered in the inner Fiskefjord. This type of amphibolite is often more fine-grained, fine banded and contains in some cases calc-silicates and/or bands/seams of quartz. The main type of the het-

erogeneous amphibolites consists of alternating layers (in most cases a few millimetres up to about five centimetres thick layers) of either mafic amphibole-rich (or ±pyroxene) layers or more felsic plagioclase-rich (and ±quartz) layers. The heterogeneous type of amphibolite is found as layers or lenses in orthogneiss and as layers in the homogeneous type of amphibolite.

Especially in the heterogeneous type of amphibolites are quartz-rich layers encountered at several localities. The quartz-content varies; from an enrichment/impregnation (silicification) of the amphibolite of probably a few percents to almost pure quartz, which in some cases may represent quartz veins/neosomes. It seems that the quartz-impregnated layers in amphibolite often are followed by a higher content of quartz veins/neosomes. In a few cases, the layers are found together with calc-silicate bearing amphibolite, but that is not the ordinary case. The quartz-rich layers are 5–75 cm thick and have in many cases a rusty brown to violet colouring on weathered surfaces. The layers are found either as distinct layers (normally thicker layers) or as several layers (normally several thinner layers) within a zone of the amphibolite sequence. Disseminated pyrrhotite and pyrite is usually encountered in the rusty brown to violet coloured layers. The sulphide content varies: normally <1 vol.%, but constitutes in some cases up to 2 vol.%. The sulphide grains are mostly ≤1 mm, but 0.5–1 cm accumulations of sulphide-grains and stringers of small sulphides (mostly 1–3 cm long) are also found. The quartz-rich amphibolite layers are also in some cases associated with high biotite and/or garnet content.

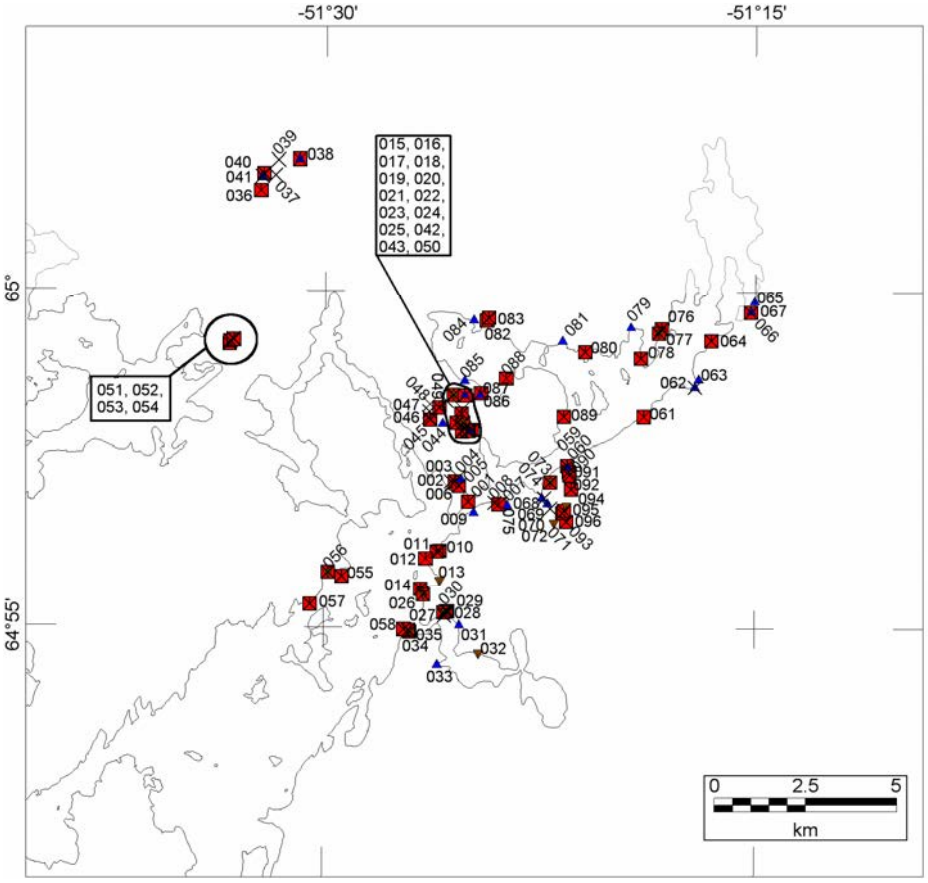

Figure 6. *Overview map of visited localities – with locality number. Prefix for the numbering is 2006bms.*

Quartz-rich sulphide-bearing layers in amphibolite was found at locality 2006bms012, -014, -017, -019, -034, -035, -036, -040, -042, -057, -064, -069, -070, -074, -076, -082 (Fig. 6). Though the layers and the localities probably represents different mineralisation types and variations within similar types, it is believed that the quartz-rich sulphide mineralised layers in many cases represent hydrothermal alteration zones with variable degrees of leaching, silicification and sulphiditisation (pyrrhotitisation), and in some cases also biotite alteration (with biotite as a product of hydrated altered amphiboles and pyroxenes) and garnetisation. However, this interpretation is only based on field observations, and should be supported by analytical work together with detailed investigations of mineral assemblages and textures. Examples of the above mentioned mineralisation in the inner Fiskefjord are seen in Figure 7.

Figure 7. *Two examples of localities with sulphide-bearing quartz-rich layers/zones in amphiblitic rocks. Left: 1–1.5 m thick massive brownish-violet layer in grey amphibolite. The layer is mineralised with disseminated pyrite, pyrrhotite, pendtlandite(?), and magnetite. The sulphides constitute c. 1-2 vol.%, however, some up to c. 5–10 cm bands within the layer consists of semi-massive to massive sulphides. The photo is from locality 2006bms034. Right: A c. 10 m wide amphibolite zone surrounded by dioritic gneisses. The amphibolite is intense quartz veined giving a wall-rock fragmentation breccia texture in places. The entire zone has a distinct yellowish colouring caused by disseminated pyrite and pyrrhotite in both the amphibolite and the quartz veins. What seems to be a flat lying fracture/crushing zone is situated just above the water level – the person for scale is standing on it. The fracture-zone is lying within what seems to be pegmatitic material. Parts/lenses (seldom more than 20 cm×20 cm × 10 cm) of the fracture zone consist of massive chert-like microcrystalline grey quartz, which contains 25–50 vol.% disseminated to semi-massive pyrite-pyrrhotite-chalcopyrite. The locality is 2006bms064.*

One of the characteristic features of the Fiskefjord region is the numerous ultramafic rock pods/lenses/bodies (with dimensions from 10 m to several 100's of meters, up to 1–2 km) which are scattered throughout the region. The ultramafic rocks are either found as isolated bodies in gneisses and amphibolite, or as part of complexes consisting of ultramafic, noritic and gabbroic rocks. The ultramafic rocks are generally dunitic peridotites; though occurrences of harzburgitic to wehrlitic compositions also occur. The ultramafic rocks are in general medium to coarse grained, with a distinct brownish-orange colouring on weathered

surfaces and a grey-greenish colouring of fresh surfaces. The rocks are massive and consist of variable amounts of mainly olivine, pyroxene and iron oxides. Serpentinisation is common in many places; either along fissures or along faults. Mica±talc±plagioclase±quartz is produced by the serpentinisation. The serpentinisation along faultplanes can be rather pervasive. Also thin veins of fibroses minerals (anthophyllite, tremolite, actinolite, etc.) are observed in some cases. Veins, network of veins and accumulations of magnetite are often seen (chromite may also be present in these veins). Isolated ultramafic bodies were visited at localities 2006bms007, -011, -051, -052, -053, -054, -058, -061, -092, -093, and -095. Ultramafic rocks as part of larger complexes of noritic rocks are found at 2006bms003, -006, and -080. The complexes are embedded within supracrustal rock sequences dominated by amphibolite or, possible, at the margin/marginal parts of such sequences.

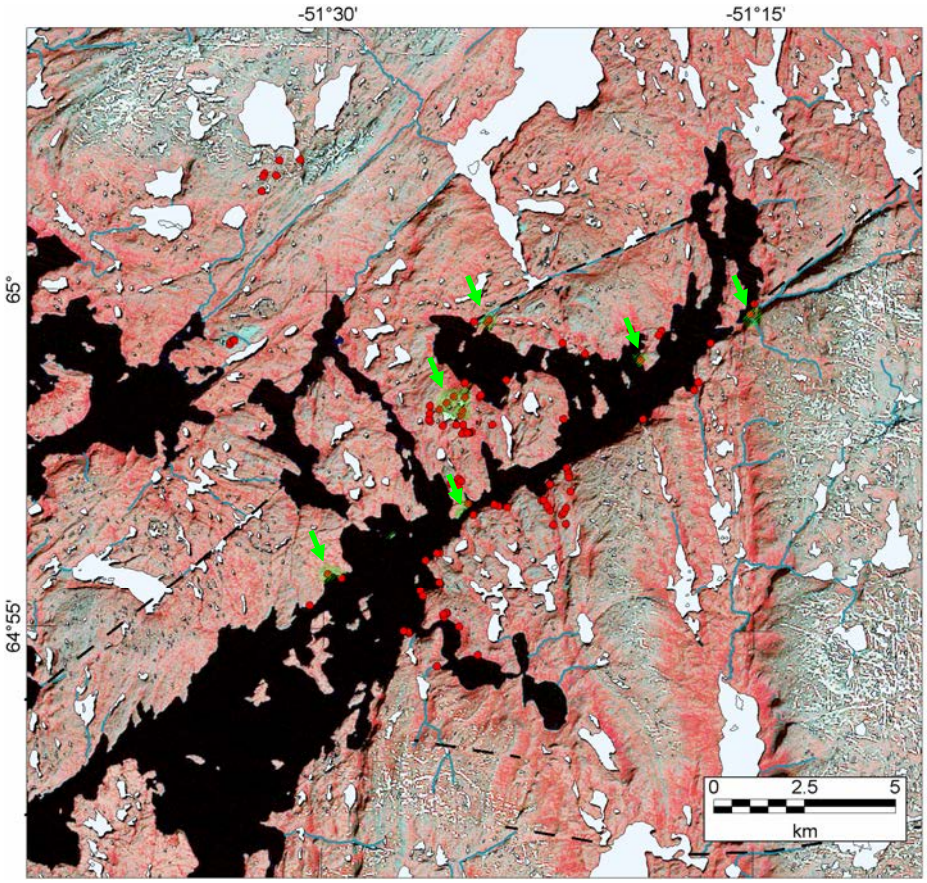

Figure 8. *Green hatches (and green arrows) indicate areas where intense epidotisation and silicification have been observed.*

Figure 9. *Photos from one of the most intense zones of epidotisation and silicification (loc. 2006BMS055). The entire zone can be followed for c. 300 m along the coast. The epidotisation causes an alteration of former quartzo-feldspathic granitic gneisses and possible amphibolite. However, primary composition of rocks are hard to judge as most of the zone consists of more or less massive epidote-quartz rock. Thin quartz veins are found throughout the zone, which also is intruded by non-altered cross-cutting pegmatites, though altered pegmatites also are present.*

A strong epidotisation, silicification and bleaching of the bedrock was observed in several zones in the inner Fiskefjord (loc. 2006bms001, -015, -022, -023, -024, -025, -055, -056, -078, -083, see Fig. 8). The epidotisation and bleaching was often found in fracture zones but massive non-fractured areas with intense epidotisations are also encountered. The latter could possible be a complete healing/replacement of the fractures by the epidote and quartz. The epidotisation causes a distinct greenish colouring of the rock; in the most intense cases, a remarkable bright green rock is created (Fig. 9). The contact between the epidotisation and the country rock seems to be transitional. Many thin quartz veins were observed in many of the epidotisised zones. Also hematisations were observed as thin hematite veins or stains at or along joint-surfaces and thin quartz veins. In most cases no sulphides were observed within the zones of epidotisation. However, sulphides were encountered at a few localities; either as small (≤1 mm) disseminated grains (<1 vol.%) in the epidotisised bleached quartz-rich rocks or as rusty patches/zones with disseminated sulphides (≤1–2 mm), accumulations of sulphides and stringers/joint fillings of sulphides in the epidotisised bleached quartz-rich rocks. The sulphides are dominated by pyrite, pyrrhotite and minor chalcopyrite, and possibly in one case (loc. 2006bms001) a few grains of arsenopyrite. An increasing number of pegmatites were often encountered at/in the the epidotised zones. In some cases it seem that the epidotisation were “developed” from the pegmatites; in other cases the pegmatites were non-altered and clearly later than the epidotisation (see Fig. 9)

As a curiosity should it be mentioned that rocks of a phlogopite-rich ultramafic lamproitic composition was found during the fieldwork in the inner part of Fiskefjord. Prior no lamproitic rocks have been located in the inner part of Fiskefjord. The rock was found at three sites along a local stream situated in a local small steep-sided N–S orientated valley with an overgrowth valley-bottom. The first occurrence (loc. 2006bms060) was located in the lowermost part of the stream just above the outlet in the fjord. This occurrence consisted of 10–12 boulders with a size from *c.* 0.2–0.4 × 0.5 × 0.5 m to *c.* 0.2–0.4 × 0.75 × 1 m. The matrix of the rock is fine-grained grey and contains a rather high amount of mica, probably phlogopite. Possible xenocrysts, up to 0.5 × 0.5 cm, of olivine(?) (pyroxenes?, ilmenite?) occur. In addition, possible fragments of presumed crustal wall rocks, gneiss, granotoid, are seen. The second occurrence (loc. 2006bms090) was located *c.* 170 m further upstream and consists of only one boulder (size 10 × 40 × 30 cm). The third occurrence (loc. 2006bms091) consisted of two boulders (0.2 × 0.5–1 × min. 0.5 m) located another 100 m upstream. It was not possible to find more boulders up stream. However, it is believed that the boulders are local of origin and that they may represent a sub-outcropping lamproitic dyke located in the small valley.

Geochemistry

Lithogeochemistry

Four out of seven representative amphibolite samples from the inner Fiskefjord plotted in a Jensen cation classification diagram falls within the upper part of the calc-alkaline field with compositions ranging from basalt to rhyolite. The three remaining samples fall within the

high-Fe and high-Mg tholeiite field. The calc-alkaline trend of amphibolites from the inner Fiskefjord is in agreement with observations made by Garde (1997), which indicated a trend from tholeiitic composition at the outer Fiskefjord towards more mixed calc-alkaline and tholeiite composition at the inner part of Fiskefjord. None of the amphibolites are sufficiently magnesian to plot in the field of komatiite composition. The amphibolites plotted in a Ti-Zr-Y discrimination diagram for different tectonomagmatic environments, three out of seven samples falls within the field for Mid-oceanic ridge basalts – Island-arc tholeiites – Calc-alkali basalts (field B in Fig. 11). One falls within the Calc-alkali basalts field and two within the within-plate basalts (field C and D in Fig. 11). One sample plots outside any classified field. The representative most unaltered amphibolite samples have REE contents at about 10 too 40 times chondritic levels with greatest variation in LREE (Fig. 12). One sample (482029) is outside the range of the other samples; this sample is also the only one which falls within the within-plate basalt field in the Ti-Zr-Y discrimination diagram. This sample may represent a metasomatised amphibolite.

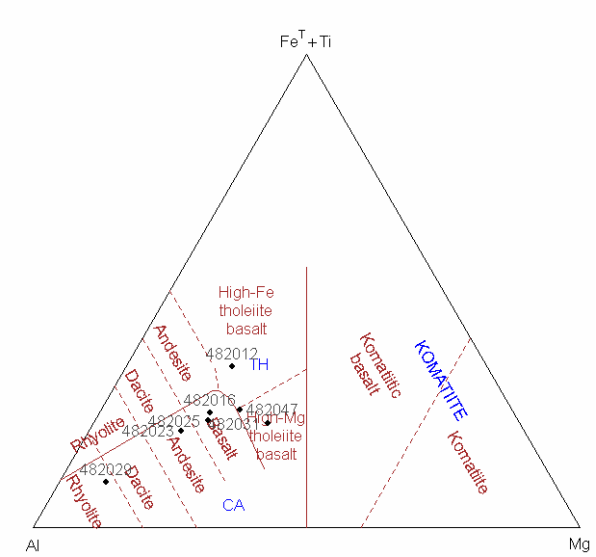

Figure 10. *Representative most unaltered amphibolite samples from the inner Fiskefjord plotted in a Jensen cation classification diagram (Jensen 1976) for volcanic rocks. The elements used in the Jensen cation classification diagram are relative insensitive with regard to loss of alkali elements during metasomatose and metamorphose.*

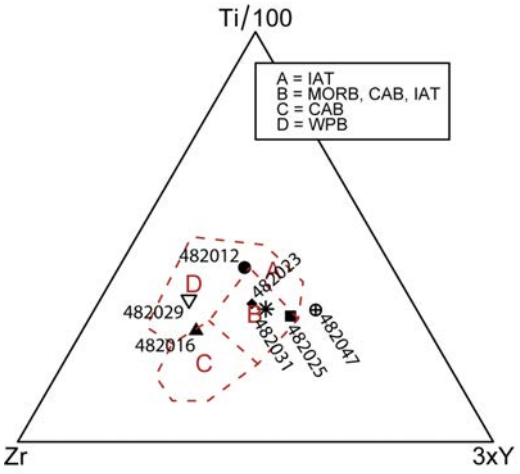

Figure 11. *Representative most unaltered amphibolite samples from inner Fiskefjord plotted in Ti-Zr-Y discrimination diagram for different tectonomagmatic environments (Pearce & Cann 1973). Abbreviations: IAT, Island arc tholeiite; MORB, Mid-oceanic ridge basalts; CAB, Calc-akali basalt; WPB, Within-plate basalts.*

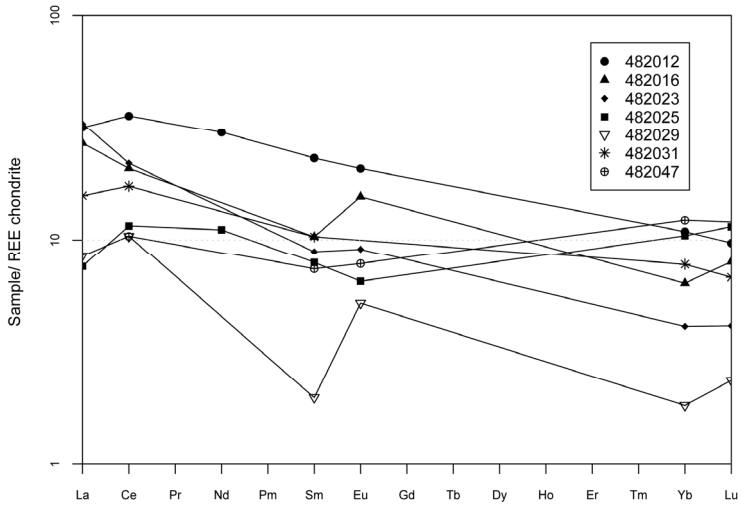

Figure 12. *Chondrite-normalised REE diagrams of the representative amphibolite samples from Fiskefjord. Chondrite values from Nakumura (1974) are used for normalisation.*

Slightly too moderately elevated gold contents with values from 7 to 377 ppb Au is encountered in several of the mineralised amphibolite sequences in the Fiskefjord area. The most notable being a sample of quartz banded/veined amphibolite, which yields 377 ppb Au together with 3 ppm As. Gold content above 10 ppb was encountered from nine different localities with three additional localities running 7 ppb Au. Altogether, it seems that rock units in the inner Fiskefjord area are slightly elevated in gold content. No elevated metal content are encountered in the epidotisised samples. Compared with the other samples from the inner Fiskefjord area, epidotisised samples are generally low in K_2O and high in Na_2O, SiO_2, and Sr (above 1000 ppm). Pinkish-white granites close to one of the epidotisised areas yields also a high Sr content.

Table 4. *Selected element concentrations of rock samples with elevated gold content from the Fiskefjord area. The selected elements shown are elevated for one or more samples with gold compared with all other samples from the area.*

Sample no.	Locality	Description	Au ppb	Ag ppm	As ppm	Co ppm	Cr ppm	Cu ppm	Ni ppm	W ppm	S pct.	MgO pct.	Ni/Mg ratio
482007	2006bms012	Rusty layer in amphibolite	39	<0.5	2	261	24	320	162	<3	5.62	1.97	136
482008	2006bms014	Contact between relative "pure" qtz.-fsp pegmatite and light-grey banded amphibolite. The contact is rusty and brownish.	35	<0.5	<2	67	197	306	155	<3	0.77	5.20	49
482009	2006bms015	Partly bleached epidote-bearing gneiss and mafic greenish fine-grained amphibolite with qtz.-rich parts/qtz. veins.	34	<0.5	<2	48	183	105	68	<3	0.24	4.37	26
482018	2006bms030	Local boulder of silicified amphibolite.	14	0.8	<2	251	317	2650	834	<3	8.44	6.82	202
482019	2006bms034	Sulphide-mineralised brown-rusty qtz.-rich amphibolite.	13	<0.5	<2	161	31	1240	224	<3	6.28	4.72	78
482039	2006bms057	Pyrrhotite-mineralised rusty amphibolite	13	<0.5	<2	105	617	70	390	<3	2.84	8.08	80
482040	2006bms057	Sulphide-mineralised sheared altered qtz. veins/bands in dark amphibolite.	377	1.1	3	59	244	358	94	56	1.12	4.61	33
482048	2006bms070	Rusty layer in amphibolite.	51	1.1	<2	168	667	3220	643	<3	4.78	5.14	207
482050	2006bms074	Qtz.-rich part/vein from rusty amphibolite with iron-sulphides.	20	0.7	<2	71	473	53	110	<3	0.35	2.79	65
482058	2006bms088	Malachite stained zone in amphibolite.	13	<0.5	<2	76	1030	229	281	<3	0.31	13.83	33
Average representative unaltered amphibolite from Fiskefjord (*n* 7) yields:			<5	<0.5	<2	48	271	88	160	<3	0.32	4.69	60

Sediment geochemistry

Six out of the 34 sediment samples (both scree and stream sediments) yields values above 10 ppb Au, with the highest being 144 ppb Au from a scree sample below a rusty part of an amphibolite sequence in a cliff-wall at locality 2006bms034. Same sample is also enriched in Cu (1100 ppm), V (456 ppm), Fe_2O_3 (25.60 %) and Ni/Mg ratio (117). Rock samples (no. 482019) from the same locality also yield gold content slightly above the background of the Nuuk region (13 ppb).

Table 5. *Selected geochemistry of collected rock and sediment samples from the inner part of Fiskefjord. Elements found to be indicative for Isua gold groups, together with other elements regarded as possible pathfinder elements for gold mineralisations or indicative for alterations are given. Enriched values are in red; elevated in blue. SSC, scree sediment sample; SSS, stream sediment sample; na, not available/analysed.*

Sample	Locality	Type	Description	Au	As	Ba	Ce	Cr	Cs	Cu	La	Ni	Pb	Rb	Sb	Sr
	2006bms-			ppb	ppm	ppm	ppm	ppm	ppm	ppm	ppm	ppm	ppm	ppm	ppm	ppm
507801	-005	SSS	SSS	< 2	< 0.5	710	75	348	< 1	34	37.8	113	13	< 15	< 0.1	697
507803	-009	SSS	SSS	< 2	< 0.5	450	54	636	3.0	64	24.7	456	37	< 15	< 0.1	354
507804	-013	SSC	SSC	17.00	< 0.5	< 50	20	410	< 1	373	9.6	308	9	< 15	< 0.1	285
507805	-016	SSS	SSS	< 2	< 0.5	420	44	203	< 1	69	21.6	94	13	36	< 0.1	441
507806	-019	SSC	SSC	< 2	< 0.5	520	75	383	< 1	193	39.3	108	21	< 15	< 0.1	363
507807	-022	SSC	Very local SSC (SSE) from scree below two-phase epidotised pegmatite.	< 2	< 0.5	560	59	145	< 1	10	27.9	61	28	65	< 0.1	969
507808	-025	SSS	SSS - local stream below cliff-wall	< 2	2.30	360	40	120	< 1	66	24.5	58	25	< 15	< 0.1	339
507809	-026	SSC	Local fresh scree sample	7.00	< 0.5	290	43	170	3.0	457	16.4	147	14	< 15	< 0.1	274
507810	-028	SSC	Local scree sample below a sequence of varying types of amphibolite	22.00	< 0.5	270	23	592	< 1	466	9.8	529	4	< 15	< 0.1	169
507811	-030	SSC	Dried-out stream in scree-fan from brownish coloured zone in amphibolite cliff-wall.	13.00	< 0.5	190	25	569	< 1	465	9.1	380	5	< 15	< 0.1	173
507812	-031	SSS	Partly dried-out stream cut in overgrown scree-fan from amphibolite sequence in cliff-wall above.	9.00	< 0.5	350	45	311	< 1	83	18.2	160	15	< 15	< 0.1	432
507813	-032	SSC	Local 10-12 m wide scree-fan from grey amphibolite sequnece with a couple of 1 m wide layer of more brownish coloured amphibolite.	12.00	< 0.5	320	22	585	< 1	325	9.0	341	11	< 15	< 0.1	196
507814	-033	SSS	A c. 5-7 m wide stream	< 2	4.00	< 50	49	193	2.0	58	29.8	114	22	< 15	0.2	411
507815	-034	SSC	Local scree sample below mineralised layer in amphibolite sequence	144.00	< 0.5	< 50	51	151	< 1	1100	17.8	262	13	< 15	< 0.1	325
507816	-041	SSS	Stream in valley - draining amphibolite, dunite and norite lithologies.	< 2	< 0.5	< 50	58	214	1.0	53	30.3	134	12	< 15	< 0.1	391
507817	-038	SSS	Stream in local distinct canyon cut in amphibolite cliff-wall. 2 order stream.	< 2	0.50	290	34	990	3.0	159	14.4	362	11	< 15	< 0.1	206
507818	-044	SSS	Local stream in small canyon with relative flat dipping sides.	< 2	< 0.5	690	121	56	< 1	28	56.3	40	20	< 15	0.4	732
507819	-056	SSC	Local scree material from crevice-fracture zone in cliff-wall. Fracture zone in strongly epidotisised granitic gneiss - some parts	7.00	< 0.5	310	140	93	3.0	13	75.4	64	7	< 15	< 0.1	1840
507820	-059	SSS	Stream draining granitic gneiss dominated area.	< 2	< 0.5	500	69	381	< 1	26	35.1	126	15	< 15	< 0.1	435
507821	-062	SSS	SSS from strong stream.	< 2	1.40	340	67	816	2.0	54	33.8	293	6	30	< 0.1	345
507822	-063	SSS	SSS from moderate-strong stream.	< 2	1.30	590	48	141	< 1	28	25.1	89	20	44	< 0.1	398
507823	-065	SSS	SSS from strong stream.	< 2	2.20	460	94	164	< 1	83	55.6	59	15	< 15	< 0.1	420
507824	-066	SSS	SSS from strong stream.	< 2	< 0.5	460	51	78	< 1	42	25.6	41	15	< 15	< 0.1	403
507825	-068	SSS	SSS from moderate to strong stream.	< 2	< 0.5	510	32	254	< 1	143	17.3	146	10	< 15	< 0.1	295
507826	-071	SSC	SSC from local fresh scree fane. Cliff-wall above scree consists of grey amphibolite, rusty-brown amphibolite layers and pegmatites.	< 2	< 0.5	< 50	26	190	< 1	238	12.0	276	6	< 15	< 0.1	187
507827	-072	SSS	SSS from moderate stream. This sample is taken 300-400 m upstream compared to 507825.	< 2	< 0.5	280	28	259	< 1	152	22.4	179	12	< 15	< 0.1	306
507828	-073	SSC	SSC from local 8 m wide scree-fan material from 1-1½ m wide rusty layer in amphibolite.	22.00	< 0.5	320	27	427	< 1	477	16.0	361	37	< 15	< 0.1	254
507830	-075	SSS	SSS from moderate 1 m wide smaller stream.	< 2	1.60	620	38	176	< 1	18	24.2	106	12	< 15	< 0.1	455
507831	-077	SSC	SSC from local 2-3 m wide scree below sulphide-mineralised amphibolite layer	< 2	< 0.5	640	49	266	< 1	622	27.1	120	17	< 15	< 0.1	247
507832	-079	SSS	SSS from moderate stream.	3.00	< 0.5	550	40	155	1.0	29	26.9	73	19	< 15	< 0.1	450
507833	-081	SSS	SSS from moderate stream.	< 2	1.30	540	38	231	< 1	37	25.0	114	14	< 15	< 0.1	447
507834	-084	SSS	SSS from strong 15-20 m wide stream.	< 2	2.60	340	50	417	2.0	81	25.2	209	12	71	< 0.1	381
507835	-085	SSS	SSS from smaller stream with weak to moderate water-flow - extension of stream at loc. 2006bms-025 (507808 SS) - fine-fraction	< 2	< 0.5	540	46	224	2.0	34	29.0	91	22	< 15	< 0.1	614
507850	-086	SSS	SSS from very small (30-50 cm wide) - not optimal, but sampled because of its location.	< 2	< 0.5	560	48	222	< 1	32	31.8	94	18	< 15	< 0.1	512
507836	-096	SSC	Small local scree from one of the many rusty-brown layers in the amphibolite at - and along the entire topographical ridge - at loc	< 2	< 0.5	< 50	63	80	< 1	334	32.0	184	10	57	< 0.1	304

Table 6. *Selected geochemistry of collected rock and sediment samples from the inner part of Fiskefjord. Continuation of* **Table 5**.

Sample	Locality	Type	V	Zn	CaO	Th	U	U/Th	Fe_2O_3	K_2O	MgO	Na_2O	S	Ni+Cr	Ni/Mg
	2006bms-		ppm	ppm	pct.	ppm	ppm	ratio	pct.	pct.	pct.	pct.	pct.	ppm	ratio
507801	-005	SSS	112	64	4.50	4.6	1.8	0.39	6.69	1.34	8.24	3.94	0.04	461	50.0
507803	-009	SSS	118	110	4.45	4.1	1.1	0.27	9.85	1.11	17.51	2.37	0.07	1092	95.0
507804	-013	SSC	321	91	7.06	0.9	< 0.5	na	13.83	0.34	11.49	2.67	0.13	718	97.8
507805	-016	SSS	198	84	4.29	2.6	< 0.5	na	8.61	1.05	7.19	2.70	0.14	297	47.7
507806	-019	SSC	201	150	3.97	8.3	1.1	0.13	10.11	2.06	9.48	3.13	0.25	491	41.5
507807	-022	SSC	120	92	5.26	2.1	< 0.5	na	6.75	1.75	7.48	3.40	0.02	206	29.8
507808	-025	SSS	82	84	2.99	2.3	< 0.5	na	6.28	0.88	3.76	1.71	0.29	178	56.3
507809	-026	SSC	447	154	6.83	0.4	0.7	1.75	22.02	0.70	8.54	2.87	0.08	317	62.8
507810	-028	SSC	287	156	7.53	0.7	< 0.5	na	13.94	0.46	15.47	1.94	0.10	1121	124.8
507811	-030	SSC	270	110	7.34	1.0	< 0.5	na	15.16	0.33	13.24	1.71	0.19	949	104.7
507812	-031	SSS	201	77	6.45	2.2	< 0.5	na	8.98	0.90	10.73	3.29	0.01	471	54.4
507813	-032	SSC	383	100	10.24	1.4	< 0.5	na	14.44	0.33	16.42	1.93	0.04	926	75.8
507814	-033	SSS	109	94	4.11	4.0	2.2	0.55	5.66	1.13	6.75	2.60	0.15	307	61.6
507815	-034	SSC	456	155	8.23	< 0.2	< 0.5	na	25.60	0.35	8.17	2.97	0.50	413	117.0
507816	-041	SSS	131	70	6.94	2.7	< 0.5	na	7.15	1.01	10.36	2.75	0.04	348	47.2
507817	-038	SSS	233	115	6.60	1.8	< 0.5	na	12.41	0.87	20.25	2.09	0.04	1352	65.2
507818	-044	SSS	169	171	4.42	2.5	< 0.5	na	10.14	1.69	9.08	2.20	0.11	96	16.1
507819	-056	SSC	162	54	12.42	5.8	1.8	0.31	10.75	0.64	7.22	2.53	0.05	157	32.3
507820	-059	SSS	98	68	4.77	5.6	2.2	0.39	6.58	1.29	9.01	3.67	0.02	507	51.0
507821	-062	SSS	110	103	4.27	4.1	< 0.5	na	8.42	0.96	15.54	2.67	0.07	1109	68.8
507822	-063	SSS	80	70	4.18	3.8	1.5	0.39	5.05	1.29	5.14	3.61	0.06	230	63.1
507823	-065	SSS	215	90	5.30	12.3	1.9	0.15	10.08	1.08	6.06	3.07	0.03	223	35.5
507824	-066	SSS	92	72	4.52	3.3	< 0.5	na	5.32	1.23	4.27	3.25	0.08	119	35.0
507825	-068	SSS	280	108	6.30	2.4	3.4	1.42	11.65	0.88	8.97	2.57	0.06	400	59.4
507826	-071	SSC	293	79	5.12	1.4	< 0.5	na	9.37	0.59	11.71	2.13	0.07	466	86.0
507827	-072	SSS	245	104	5.60	1.7	4.9	2.88	9.25	1.05	8.43	2.45	0.08	438	77.5
507828	-073	SSC	232	348	5.76	2.2	< 0.5	na	12.16	0.49	14.77	2.83	0.06	788	89.1
507830	-075	SSS	88	63	4.25	3.0	6.2	2.07	5.32	1.08	5.73	3.40	0.06	282	67.5
507831	-077	SSC	162	154	2.74	6.6	3.2	0.48	16.59	2.16	8.28	2.20	1.44	386	52.9
507832	-079	SSS	106	96	4.74	3.9	1.4	0.36	5.02	1.43	6.35	3.28	0.04	228	42.0
507833	-081	SSS	115	84	4.50	4.1	< 0.5	na	5.68	1.51	7.15	3.32	0.04	345	58.2
507834	-084	SSS	200	119	5.72	3.8	< 0.5	na	9.34	1.10	15.32	2.59	0.07	626	49.8
507835	-085	SSS	95	77	4.52	4.5	< 0.5	na	5.29	1.74	7.88	3.49	0.05	315	42.1
507850	-086	SSS	91	66	4.13	5.1	1.9	0.37	4.92	1.34	6.89	3.33	0.07	316	49.7
507836	-096	SSC	393	148	7.86	< 0.2	< 0.5	na	16.02	0.72	7.55	3.01	0.02	264	89.0

Qooqqut Lake (area 2)

Characteristic signatures of the favourable areas

The top 0.5% and 1.5% most favourable area for the Storø group in the vicinity of Qooqqut Lake is characterised by high content of Al_2O_3, Cs, La, Ni/Mg ratio, Th and U in the fine fraction stream sediment geochemistry (Fig. 13 and Table 7). Aeroradiometric K and eU/Th is characterised by being considerable higher than the mean for the entire study region.

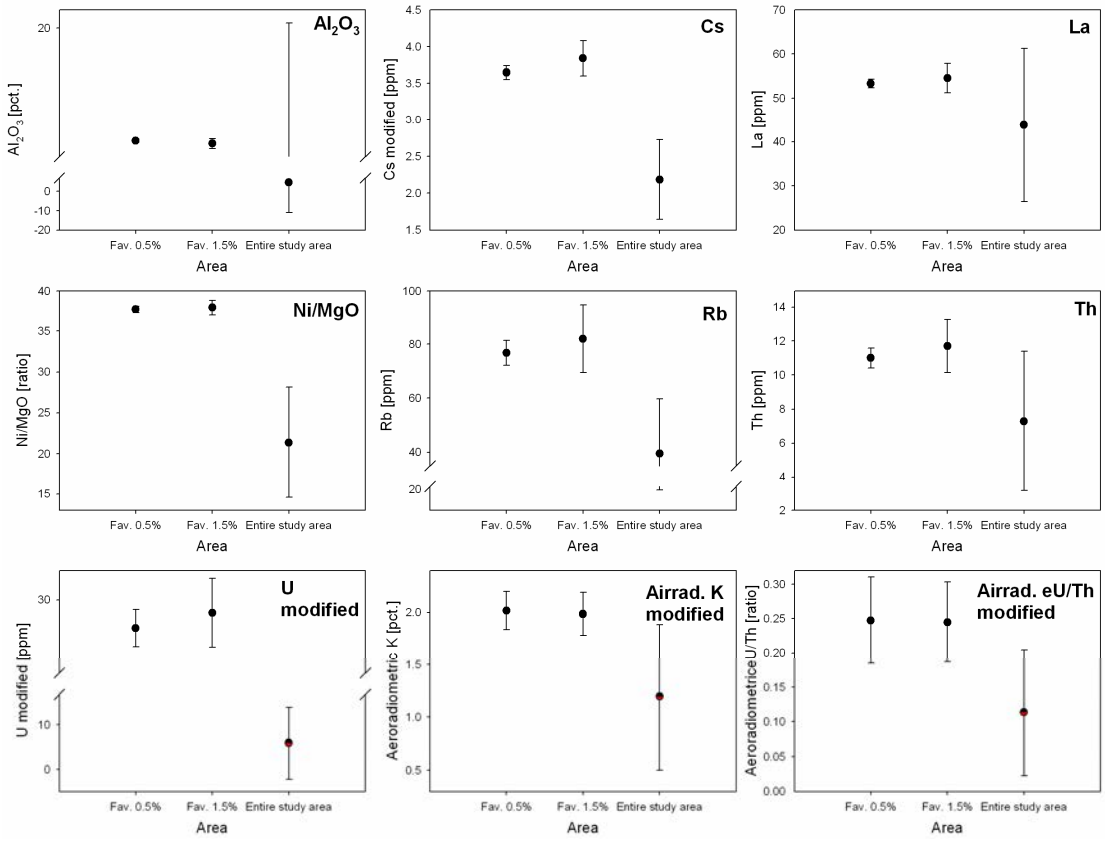

Figure 13. *Plot of the mean values and associated standard deviation extracted from different data sets for the top 0.5% and 2.5% most favourable area (Fig. 14) for gold showings of the Storø group (Nielsen et al. 2004; Stensgaard et al. 2006b) in the vicinity of Qooqqut Lake. The values are also given in Table 7. See Figure 4 for symbol and colour legend.*

Table 7. *Extracted mean data values and standard deviation of the gridded data found to be characteristic for the Storø group of gold showings (Stensgaard et al. 2006b). The extracted values are for the top 0.5% and 1.5% most favourable areas (see Fig. 3) near Qooqqut lake.*

Area	Mean Al_2O_3 [pct.]	StdDev. Al_2O_3	Mean Cs modi [ppm]	StdDev. mean Cs modi.	Mean La [ppm]	StdDev. La	Mean Ni/Mg [ratio]	StdDev. Ni/Mg
0.5%	13.85	0.08	3.65	0.10	53.31	0.94	37.63	0.38
1.5%	13.69	0.27	3.84	0.24	54.55	3.32	37.86	0.90
Entire study area	4.67	15.60	2.18	0.54	43.80	17.42	21.38	6.77
Area	**Mean Rb [ppm]**	**StdDev. Rb**	**Mean Th [ppm]**	**StdDev. Th**	**Mean U modi. [ppm]**	**StdDev. U modi.**	**Mean airrad. eU/Th [ratio]**	**StdDev. airrad. eU/Th**
0.5%	76.75	4.69	11	0.58	28.08	1.28	2.02	0.18
1.5%	81.95	12.50	11.71	1.55	29.11	2.36	1.99	0.21
Entire study area	39.56	20.22	7.28	4.11	5.89	8.13	1.19	0.69

Geological observations

An up to c. 100 m wide sequence of supracrustal rock is located in the western cliff-wall of the valley of Qooqqut lake (Figs 14 and 15, locality 2006bms120). The area was also visited briefly by Henrik Stendal, GEUS, in 2005 (Hollis *et al.* 2006b). However, his work was concentrated to the southwestern part of the valley at Qooqqut lake. Relicts of deformed pillows were encountered during the 2005 fieldwork in exposed amphibolite at the main stream draining the lake towards southwest.

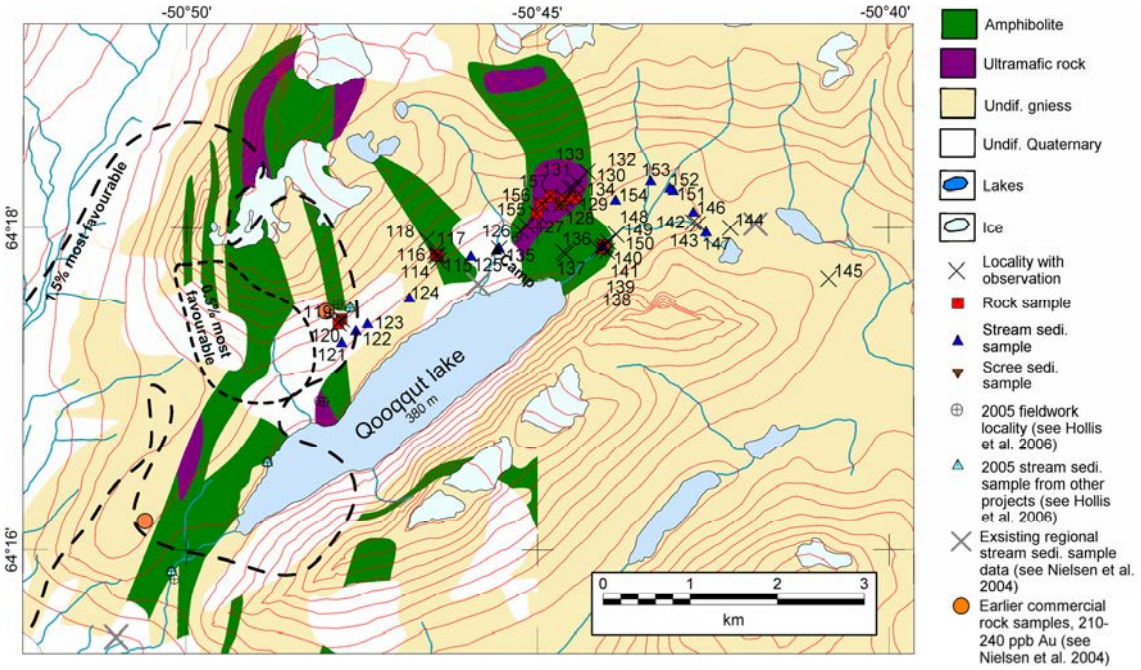

Figure 14. *Geological map for the area around Qooqqut lake with position of visited localities and samples. Geology west of 50°45' is taken from the digital version (Hollis et al. 2006b) of the Qôrqut 1:100 000 map sheet (McGregor 1983). Amphibolite and ultramafic units east hereof are based on mapping made by the author during the fieldwork. Locality numbers are given in black. The outline of the 0.5% and 1.5% most favourable area is based on the favourability map for Storø group gold showings utilising the distribution of Al_2O_3, Cs, La, Rb, Th, U, and Ni/Mg in*

the fine fraction regional stream sediment geochemistry and the concentrations of K and eU/Th calculated from the aeroradiometric data.

Table 8. *Overview of samples from the different localities in the Qooqqut area.*

Locality	Rock sample	Locality no.	Stream sediment sample no.
2006bms115	482078	2006bms121	507844
2006bms116	482079	2006bms122	507845
2006bms119	482080	2006bms123	507846
2006bms120	482081	2006bms124	507855
2006bms128	482082	2006bms125	507856
2006bms128	482083	2006bms135	507858
2006bms129	482084	2006bms146	507860
2006bms134	482085	2006bms147	507859
2006bms139	482086	2006bms150	507861
2006bms140	482087	2006bms151	507862
2006bms140	482088	2006bms152	507863
2006bms155	482089	2006bms153	507864
2006bms156	482090	2006bms154	507865
2006bms157	482091	**Locality**	**Scree sediment sample no.**
		2006bms119	507840
		2006bms128	507857

Figure 15. *Amphibolite sequence with rusty layers in the northwestern cliff-wall of the Qooqqut lake valley. From distance, it seems that the sequence is deformed/strained. Samples from the local scree fan below the sequence are taken. Photo: Henrik Stendal, GEUS, 2005.*

In the central and western part on the northern shore of the Qooqqut lake, the amphibolite sequence is intercalated with the Amitsoq gneisses and intruded by the Ikkattoq gneisses. The majority of the sequence here consists mainly of a regular fine- to medium-grained fine banded grey coloured mafic amphibolite. As the best exposure of the amphibolite sequence is located in the non-accessible steep cliff-wall the local boulder-scree fan below was sampled. Quartz-rich amphibolite parts/layers, which probably represent silicification, are encountered in many massive rusty-violet boulders. Quartz veins are also observed in these boulders. Chlorite and garnet is present in some of the quartz-rich rocks. These boulders originate from similar coloured layers/zones in the amphibolite in the cliff-wall. Up to 3–5

vol% disseminated discrete scattered pyrrhotite+pyrite±chalcopyrite grains (seldom larger than 1 mm) and accumulations (up to 0.5–1 cm) of such grains are present in many of the quartz-rich boulders. Similar rock and mineralisations types have been described from fieldwork in 2005 by Henrik Stendal, GEUS (Hollis *et al.* 2006b).

The area in the northeastern end of the valley at Qooqqut lake is dominated by an amphibolite sequence, which is intercalated with a large complex of ultramafic rocks. An up to *c.* 20–30 m wide and *c.* 300 m long lens of altered amphibolite is located in the centre of the complex (loc. 2006bms128, -129, -130, -131, -132). The amphibolite lens is rusty-brown with violets parts (Fig. 16), and is silicified throughout and disseminated with up to 5 vol% iron sulphides (pyrite+ pyrrhotite). Towards the sides of the lens the amphibolite becomes generally more coarse grained and a zone with larger crystals (1–2 cm) of amphiboles(?) are seen. This could be an effect of recrystallisation along the rims of the lens. A smaller amphibolite (10–20 m x ~100 m) is located southwest of the lens.

Sheets and pegmatites of the Qôrqut granite complex are numerous in the entire area.

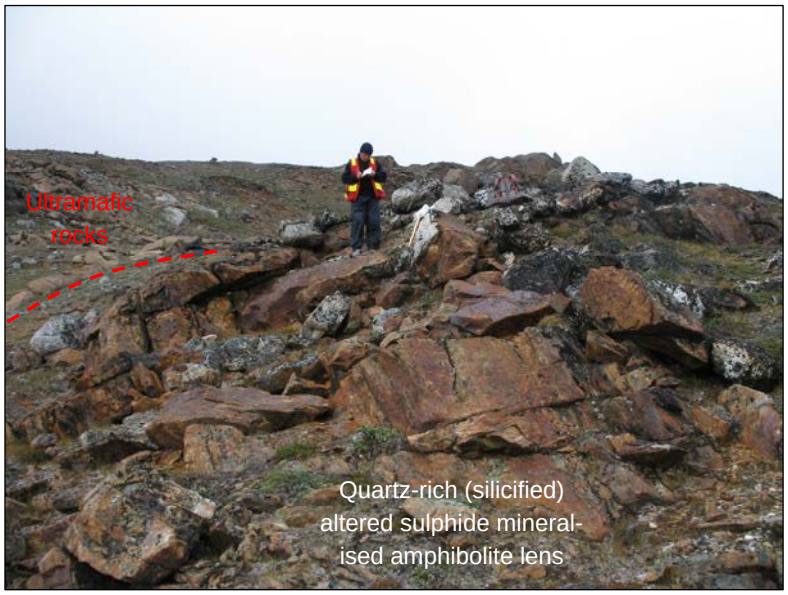

Figure 16. *Part of the silicified and sulphide mineralised amphibolite lens within ultramafic rocks (loc. 2006bms129; sample no. 482084).*

Figure 17. *Part of the silicified and sulphide mineralised amphibolite lens within ultramafic rocks (loc. 2006bms128; sample no. 482083)*

The ultramafic rocks comprise many different textures – fine grained and coarse-grained massive homogeneous non-layered forms to more fine-grained and coarse-grained heterogeneous layered forms. In addition, the magnetite content and the morphology of the magnetite vary from one part of the complex to another. Some parts only contains non to very small amounts of magnetite – disseminated, in seams or in thin bands, whereas other parts of the complex (layers, zones, lenses – mostly up to a couple of metres wide and traceable tens of metres) contains abundant magnetite as disseminated grains, veins/bands (Fig. 18) and accumulations of magnetite in patches. Much of the magnetite in veins, band and accumulated patches rich in magnetite is probably a product of hydrothermal alteration. This could also be the case for the disseminated forms, but the magnetite could also be a primary form.

Figure 18. *Network of magnetite bands/veins in ultramafic rocks.*

A quartz band parallel to the foliation (uncertain if the band represents a strongly silicified layer in the amphibolite or quartz vein intruded parallel to the foliation, 10–30 cm wide) are found within the fine- to medium-grained grey mafic amphibolite at locality 2006bms140 (Fig. 19) in the stream northeast of the end of Qooqqut lake. The amphibolite has a platy appearance. The quartz is laminated with thin bands/seams of greenish (chlorite?) and darker blackish minerals (amphiboles?). Disseminated pyrite, chalcopyrite and pyrrhotite are scattered in the quartz (grains mostly <1 mm, some 1–2 mm). Small mm-stringers (5–10 mm long) of sulphides are also found. The sulphides constitute less than 1 vol.%. The quartz is foggy-greyish-white.

Figure 19. *Photo-panorama of 10–30 cm thick sulphide bearing laminated quartz vein/layer (outlined with red dashed line) in platy grey mafic amphibolite. Strike of foliation is 60°, dip 40°SE. Inset photo taken towards ENE along the strike of the amphibolite and the parallel quartz layer/vein.*

Geochemistry

Lithogeochemistry

Two out of three representative amphibolite samples from the area around Qooqqut lake falls within the high-Mg and high-Fe tholeiite field in a Jensen cation classification diagram (Fig. 20), the third sample falls in the basalt field, close to the separation line to the high-Mg field. In the geotectonic discrimination diagram of Pearce & Cann (1973) all samples falls within mixed Mid-oceanic ridge basalts–Island Arc tholeiite–calc-akali basalt field.

The most notable metal content encountered in the Qooqqut area is within the fine-banded altered quartz-rich and quartz-veined amphibolite rocks intercalated with ultramafic rocks at

locality 2006bms129 and -128, -130, -131, -132 (see Figs 16 and 17). Selected metal content from this rock is given in Table 9.

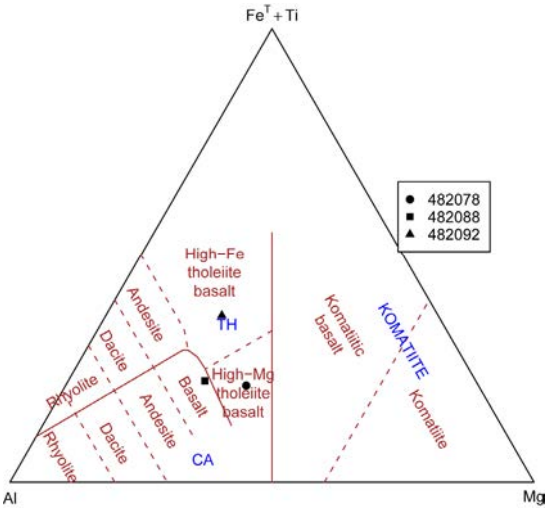

Figure 20. *Representative most unaltered amphibolite samples from the Qooqqut lake area plotted in a Jensen cation classification diagram (Jensen 1976) for volcanic rocks. The elements used in the Jensen cation classification diagram are relative insensitive with regard to loss of alkalis during metasomatose and metamorphose. TH indicates the tholeiite field, CA the calc-alkaline field.*

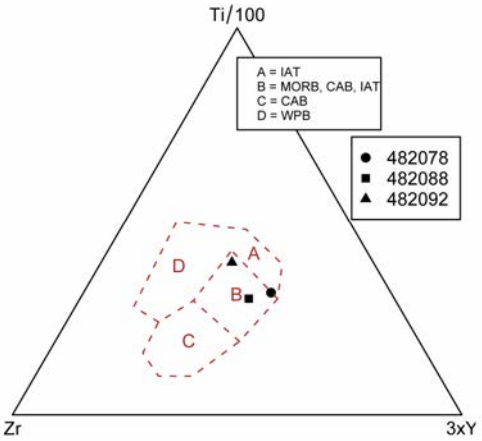

Figure 21. *Representative most unaltered amphibolite samples from Qooqqut lake area plotted in Ti-Zr-Y discrimination diagram for different tectonomagmatic environments (Pearce & Cann 1973). See Figure 11 for abbreviations.*

Table 9. *Selected metal content in altered quartz-mica rich amphibolite in the northeastern Qooqqut lake area.*

Sample no.	Locality	Description	Zn %	Pb ppm	Au ppb	Cu ppm	Cr ppm	Co ppm	Ni ppm	Cd ppm	Ce ppm	Eu ppm	Ni/Mg
482082	2006bms128	Bleached qtz-mica rich amphibolite	0.061	23	<5	903	169	147	748	1.3	45	1.7	446
482083	2006bms128	Fine-grained qtz-rich band from amphibolite	0.387	57	<5	486	1160	109	790	15.9	32	1.6	116
482084	2006bms129	Fine-grained qtz. (vein?) with thin bands of more darker bands (amphi-boles?)	1.580	46	<5	2040	164	245	1240	59.3	48	1.5	482

The mineralised amphibolites from the northeastern part of Qooqqut are anomalous Zn, Cu, Cr and Ni and elevated in elevated in Pb, Cd, Ce, and Eu compared to other non-mineralised and mineralised from the Qooqqut area and the other areas visited in 2006. The Zn-bearing amphibolite (sample no. 482084) also constitutes the highest Ni/Mg ratio encountered in the samples from 2006.

The central and western part of the Qooqqut lake area have formerly yielded elevated gold contents of 200–380 ppb Au (Stensgaard *et al.* 2004). It was not possible to duplicate such values from the samples taken during the 2006 fieldwork.

Magnetite-bearing ultramafic rocks from the northeastern Qooqqut was tested for PGE' but yielded no notable high metal concentrations (see Table 10)

Table 10. *Selected element concentrations for ultramafic rocks from the northeastern Qooqqut lake area. The elements Cr, Co, Ni, Bi and MgO are all enriched compared with other samples taken during the 2006 fieldwork, but they are not unusually high for ultramafic rocks.*

Sample no.	Locality	Description	Cr ppm	Co ppm	Ni ppm	Au ppb	Pd ppb	Pt ppb	Bi ppm	Fe_2O_3 pct.	MgO pct.
482089	2006bms155	Ultramafic rock with magnetite veins.	2280	104	1300	4	6	4.7	39	10.55	28.20
482090	2006bms156	Ultramafic rock - magnetite rich.	1540	76	442	2	5.7	7.6	27	10.82	20.53
482091	2006bms157	Ultramafic rock - magnetite rich.	2750	114	1460	<1	4.2	5.4	39	10.35	32.39

Sediment geochemistry

All sediment samples from the Qooqqut area are enriched in Th (max 15.3 ppm) and U (max 35.7 ppm). This confirms that the Qooqqut area is part of the enriched U and Th tract already defined from both aeroradiometric and stream sediment geochemistry data (see e.g., Appel *et al.* 2005; Steenfelt 1987; Steenfelt 1990). Nevertheless, based on the geo-chemistry is it not possible to make a clear verification of the areas potential for gold.

Table 11. *Selected geochemistry of collected rock and sediment samples from the Qooqqut area. Elements found to be indicative for Storø gold groups, together with other elements regarded as possible pathfinder elements for gold mineralisations or indicative for alterations are given. Enriched values are in red; elevated in blue. SSC, scree sediment sample; SSS, stream sediment sample; na, not available/analysed.*

Sample	Locality	Type	Description	Au	As	Ba	Ce	Cr	Cs	Cu	La	Ni	Pb	Rb	Sb
	2006bms-			ppb	ppm	ppm	ppm	ppm	ppm	ppm	ppm	ppm	ppm	ppm	ppm
507855	-124	SSS	SSS from c. ½–1 m wide dried-out stream.	< 2	< 0.5	450	54	193	3	36	32.90	100	26	52	0.3
507856	-125	SSS	SSS from c. 1 m wide moderate stream.	< 2	< 0.5	580	65	184	3	43	57.70	98	26	50	< 0.1
507857	-128	SSC	SSC of fine-fraction material from 15 m section across the amphibolite lens - local scree material.	< 2	< 0.5	550	37	739	4	496	19.40	334	25	< 15	< 0.1
507858	-135	SSS	SSS from 10–12 m wide strong stream.	9	< 0.5	530	79	207	3	54	39.10	120	27	51	0.3
507859	-147	SSS	SSS from moderate stream, 1-4 m in granitic gneiss.	< 2	2.10	450	71	108	< 1	29	35.70	56	24	< 15	0.3
507860	-146	SSS	SSS from smaller 0.7–1 m wide weak stream.	< 2	< 0.5	430	58	99	2	30	56.10	49	18	83	< 0.1
507861	-150	SSS	~10–12 m wide moderate to strong stream in valley bottom.	< 2	1.30	360	62	144	2	27	37.40	70	22	< 15	< 0.1
507862	-151	SSS	Small 0.3–0.5 m wide weak stream.	< 2	< 0.5	320	54	108	< 1	16	34	45	18	48	< 0.1
507863	-152	SSS	Small 1 m wide weak to moderate stream.	< 2	< 0.5	480	61	99	< 1	19	31.50	46	21	51	< 0.1
507864	-153	SSS	SSS from 2–4 m moderate to strong stream.	< 2	< 0.5	640	119	207	4	38	46.80	73	27	< 15	< 0.1
507865	-154	SSS	SSS from small 0.5 m wide weak stream.	< 2	1.50	500	75	171	4	54	73.10	103	25	78	< 0.1

Sample	Locality	Type	Description	Sr	Zn	Th	U	U/Th	Al_2O_3	Fe_2O_3	K_2O	MgO	S	Ni+Cr	Ni/Mg
	2006bms-			ppm	ppm	ppm	ppm	ratio	pct.	pct.	pct.	pct.	pct.	ppm	ratio
507855	-124	SSS	-see above	323	51	8.6	1.6	0.19	10.67	4.38	1.78	5.76	0.03	293	63.3
507856	-125	SSS	-see above	314	52	6.4	8.5	1.33	9.62	4.70	1.77	5.58	0.04	282	64.1
507857	-128	SSC	-see above	166	318	5.4	2.2	0.41	9.07	16.59	1.57	16.49	0.44	1073	74.0
507858	-135	SSS	-see above	298	67	10.2	13.6	1.33	10.30	5.31	1.89	6.71	0.03	327	65.2
507859	-147	SSS	-see above	351	50	8.5	11.9	1.40	9.31	4.48	1.75	4.34	0.05	164	47.1
507860	-146	SSS	-see above	340	54	7.1	20.4	2.87	8.33	3.85	1.70	3.83	0.04	148	46.7
507861	-150	SSS	-see above	337	56	8.5	9.4	1.11	7.82	5.09	1.64	4.71	0.02	214	54.3
507862	-151	SSS	-see above	329	42	6.0	11.1	1.85	8.58	4.00	1.51	3.90	0.03	153	42.1
507863	-152	SSS	-see above	341	49	6.6	6.9	1.05	9.22	4.15	1.71	4.05	0.03	145	41.4
507864	-153	SSS	-see above	317	62	15.3	7.5	0.49	8.54	7.09	1.76	5.29	0.02	280	50.3
507865	-154	SSS	-see above	274	54	8.4	35.7	4.25	8.29	4.36	1.82	4.96	0.06	274	75.7

Serfarsuit (area 3)

Geological observations

This area comprises an up to 1 km wide amphibolite sequence of both homogenous banded fine grained amphibolite with alternating darker bands rich in amphiboles and grey to white bands of more intermediate to felsic composition (Figs 22 and 23), in some cases with calc-silicate alteration in bands, augens or lenses (Figs 24 and 25). Felsic quarts-rich melt veins parallel to the foliation of the amphibolite or as crosscutting veins are frequent.

Figure 22. *Fine-grained and fine-banded regular amphibolite (loc. 2006bms158).*

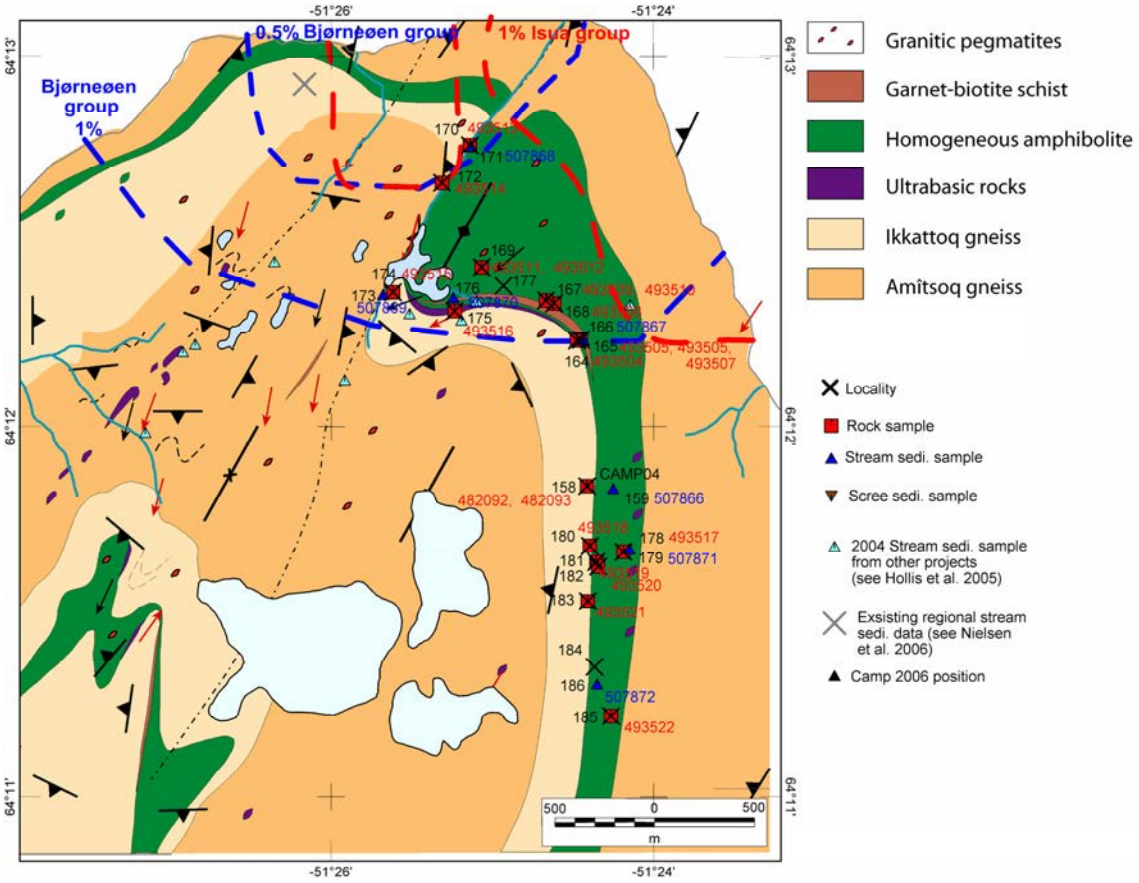

Figure 23. *Modified geological map of the Serfarsuit area (Hollis et al. 2004) with positions of localities and samples. Small ice-caps are shown in light turquoise and lakes are shown in light blue. Three-digit locality number is given in black, rock sample number in red and stream sediment sample number in blue. No scree sediment samples have been taken in the Serfarsuit area.*

Figure 24. *Calc-silicate bands in fine-grained banded amphibolite (loc. 2006bms165).*

The entire area is crosscut and divided by a great number of voluminous, up to 10 m thick, granite and coarse-grained quartz-plagioclase dominated sheets and veins. Heterogeneous garnet-biotite layers (Fig. 26, mostly a couple of metres wide, but in one case up to 15–20 m), and garnetite layers/lenses (width up to a few metres, however mostly less than 1 m, length up to 10–15 m) intercalated in the amphibolites are found in the southwestern part of the Serfarsuit area (e.g. locality 2006bms168). These were interpreted as metavolcanic by Hollis *et al.* (2004), which is supported by their close association with amphibolite units. Observations made under the fieldwork in 2006 are in agreement with this interpretation. Lenses and layers of meta-ultrabasic rocks occur at the top and bottom rim-zone of the amphibolite sequence along the contact to the Ikkattoq and Amitsoq gneiss. The lenses form bodies that are up to 10–20 m wide and up to 100 m long. Relict, coarse-grained igneous textures is observed in places.

Figure 25. *A c. 1½ × 12 m calc-silicate lens in banded amphibolite relative felsic in composition (loc. 2006bms185).*

Figure 26. *Garnet-biotite schist with some melt-veins parallel to foliation.*

Disseminated pyrrhotite ± pyrite (in most cases ≤1 mm grains) is found in many places in rusty-brownish often silicified quartz-rich layers in the amphibolite. The layers are in most cases less than 1 m thick and can be followed for tens of metres. In many cases, it seems that these layers are found near amphibolite with increased content of quartz rich melt veins and/or granitic sheets. Biotite and garnets in the layers were encountered in several cases – a possible indication of alteration processes.

Figure 27. *Typical rusty-brown sulphide-mineralised layer in amphibolite (loc. 2006bms158). In this case, directly below c. 2 m thick granitic sheet (above person). Red frame indicate the approximate area of the inset photo taken from another angle.*

Only at one locality was intense small-scale isoclinal folding internal in the amphibolite observed. Several rusty quartz-rich layers (also folded) intensely mineralised (pyrite) are situated within the folded amphibolite (Fig. 28). The folded amphibolite constitutes 10 m, which is in between two large granitic-pegmatitic vertical dipping sheets. Outside the folded amphibolite and the the sheets, the amphibolite sequence obtains its flat lying regular foliation. The amphibolite becomes very mica-rich (biotite, muscovite – a possible indication of hydratisation reactions such as seriticitisation) towards the larger more pegmatitic sheet to the northwest (Fig. 28).

Towards northwest the amphibolite sequence in Serfarsuit area is cut by a 20° orientated fault zone (Fig. 29). In some parts, the zone shows characteristics of protomylonitic textures, whereas the main part of the zone shows fractured crushed characteristics of a brittle nature. The fault zone is probably formed under brittle-ductile conditions, or reactivated under brittle conditions. The fault zone is *c.* 20 m wide and bleached due to hydrothermal

activity. Hematite veins (≤1 cm thick) and coatings on small-scale joint fractures are found throughout the zone. Fine- to medium-grained, in some places microcrystalline, quartz layers (½-1½ m thick) are found at several localities within the zone. Seams and bands (1–2 mm thick) of darker blackish and greenish minerals (amphiboles?, chlorite?) are found within the quartz. Whereas the fine- to medium-grained quartz has a rusty brownish colouring, the microcrystalline quartz layers have a distinct yellowish powdery coating on weathered surfaces. Disseminated pyrite and pyrrhotite (≤1 mm grains and constitute less than 1 vol%) are found in many of the rusty quartz layers.

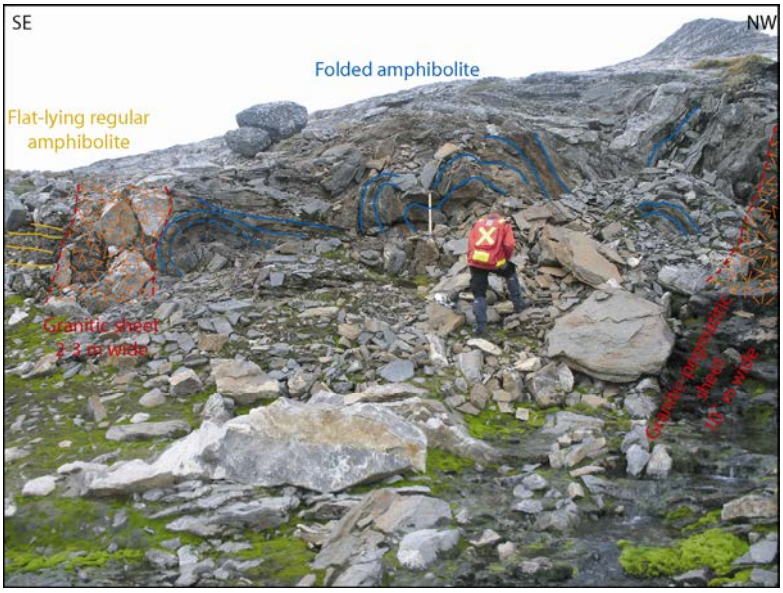

Figure 28. *Folded amphibolite with rusty layers with disseminated pyrite (loc. 2006bms181).*

Figure 29. *Fault zone cutting the amphibolite sequence in the northwestern part of the Serfarsuit area (loc. 2006bms170) – the central fault-plan is running in the snow covered fault gorge. Rusty quartz layer is seen in the NW-wall of the fault zone. Godthaabsfjord is seen in the background towards NE, with Sermitsiaq to the west and Storø to the east.*

Geochemistry

Lithogeochemistry

Four out of five representative most unaltered amphibolite samples plotted in a Jensen cation classification diagram (Jensen 1976) all falls within the High-Fe tholeiite basalt field, the fifth sample falls within the High-Mg tholeiite basalt field (Fig. 30). When plotted in a geotectonic discrimination diagram (Pearce & Cann 1973) three of the amphibolite samples fall within the field for Mid-oceanic ridge basalts – Island Arc tholeiites – Calc-alkali basalts field and two within the Within-plate basalt field (Fig. 31).

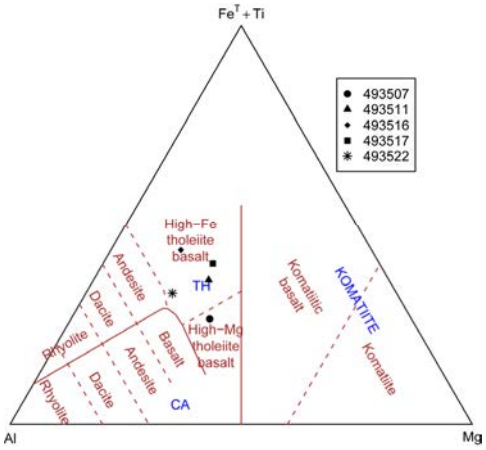

Figure 30. *Representative most unaltered amphibolite samples from the Serfarsuit area plotted in a Jensen cation classification diagram (Jensen 1976) for volcanic rocks. See Figure 20 for abbreviations.*

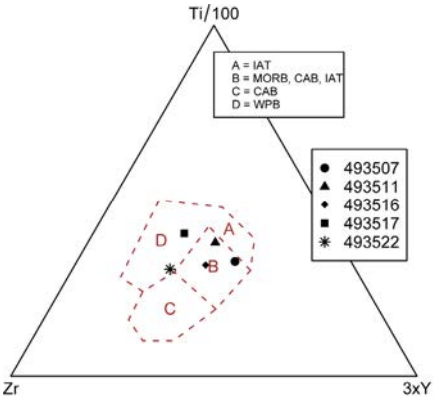

Figure 31. *Representative most unaltered amphibolite samples from Serfarsuit area plotted in Ti-Zr-Y discrimination diagram for different tectonomagmatic environments (Pearce & Cann 1973). See Figure 11 for abbreviations.*

The gold content in a light-brownish quartz-rich biotite-garnet schist (loc. 2006bms168), which in parts is almost a garnetite yielded 11 ppb Au and a sample from a quartz-rich (silicified) transition zone between a homogeneous and heterogeneous amphibolite yielded 8 ppb Au (loc. 2006bms169).

Sample of quartz layer with thin dark mineral seams/bands and distinct yellowish weathering surfaces from within a pronounced brittle fault zone in Ikkattoq gneiss and amphibolite yielded 10 ppm As (sample 493513, loc. 2006bms170). Another sample within the fault zone (loc. 2006bms172, 300 m southwest of former locality) yielded 4 ppm As. A sample of homogen sulphide-bearing amphibolite layer with small amounts of disseminated iron-sulphides yields 3 ppm As. Detectable arsenic is seldomly encountered within supracrustal successions in the Nuuk region (Hollis *et al.* 2004) and a distinct correlation between highly anomalous arsenic with the gold occurrences at Storø has been established (Stensgaard *et al.* 2006b). This makes the obtained arsenic content at Serfarsuit notable despite the samples cannot be described as strongly enriched in arsenic.

Sediment geochemistry

Four out of nine stream sediment samples confirm the slightly elevated arsenic content observed in the rock samples from the Serfarsuit area. Furthermore, as for the Qooqqut area is enrichment in radioelement Th and U, and for the Serfarsuit area also K, observed. This confirms that the Serfarsuit area is part of the tract with elevated radioactivity already defined from both aeroradiometric and stream sediment geochemistry data (see e.g., Appel *et al.* 2005; Steenfelt 1987; Steenfelt 1990). However, despite the verification of these characteristics for the Serfarsuit area, it is not possible to make a clear verification of a signature similar to that defined for the gold groups.

Table 12. *Selected geochemistry of collected rock and sediment samples from the Serfarsuit area. Elements found to be indicative of the Isua and Bjørneøen gold groups, together with other elements regarded as possible pathfinder elements for gold mineralisations or indicative for alterations are given. Enriched values are in red; elevated in blue. SSS, stream sediment sample.*

Sample	Locality	Type	Description	Au	As	Ba	Ce	Cr	Cu	La	Ni	Pb	Rb	Sb	Sr
	2006bms-			ppb	ppm	ppm	ppm	ppm	ppm	ppm	ppm	ppm	ppm	ppm	ppm
507866	-159	SSS	~2~3 m moderate stream	< 2	< 0.5	420	74	144	35	34.0	70	37	<15	< 0.1	246
507867	-166	SSS	SSS from 1–3 m wide small weak stream.	< 2	2	430	85	144	52	38.3	69	37	84	< 0.1	250
507868	-171	SSS	SSS from 1–2 m wide stream in fault-crevasse.	< 2	2	470	77	108	37	33.2	62	53	82	0.3	284
507869	-173	SSS	SSS from 3 m wide moderate stream.	< 2	1	260	94	189	41	42.5	108	37	55	< 0.1	261
507870	-176	SSS	SSS from 5–8 m wide flat stream.	6	2	370	71	153	68	32.3	113	37	65	< 0.1	264
507871	-178	SSS	SSS from 2–3 m wide flat weak to moderate stream.	< 2	2	410	68	135	53	30.6	76	35	82	< 0.1	275
507872	-186	SSS	SSS from small weak stream.	< 2	< 0.5	460	75	153	52	36.5	83	31	85	< 0.1	255

Sample	Locality	Type	Description	Zn	Th	U	U/Th	CaO	Fe_2O_3	K_2O	MgO	Na_2O	S	Ni+Cr	Ni/Mg
	2006bms-			ppm	ppm	ppm	ratio		pct.	pct.	pct.	pct.	pct.	ppm	ratio
507866	-159	SSS	- see above	60	8.4	10.2	1.2	4.02	4.69	2.07	5.18	3.1	0.03	214	49.3
507867	-166	SSS	- see above	61	11.9	20.4	1.7	3.60	4.88	2.43	4.78	3.1	0.04	213	52.7
507868	-171	SSS	- see above	65	9.4	11.9	1.3	4.24	4.83	2.21	4.56	3.1	0.03	170	49.6
507869	-173	SSS	- see above	85	8.0	6.5	0.8	4.59	5.78	1.95	6.46	2.9	0.02	297	61.0
507870	-176	SSS	- see above	80	7.2	9.4	1.3	4.49	5.76	1.94	7.22	2.8	0.03	266	57.0
507871	-178	SSS	- see above	59	8.5	8.3	1.0	4.32	4.68	2.24	5.11	3.1	0.03	211	54.3
507872	-186	SSS	- see above	61	9.4	4.6	0.5	3.93	4.86	2.25	5.73	3.1	0.02	236	52.9

Favourability for gold – follow-up by reconnaissance

As a part of the follow-up on areas outlined as most favourable, a one-day helicopter reconnaissance program was carried out. The objectives with the reconnaissance were to see if short geological visits and collection of new samples could be used to target and verify the statistical results in areas where no prior information on mineral occurrences existed.

Outer Fiskefjord – reconnaissance stop A (area 4)

Outer Fiskefjord is predicted as belonging to the most gold favourable area for the Isua gold group. A small part of the most favourable area was visited during a short reconnaissance stop. It should be noted, that the stop was located in the outer part of the area predicted as being most favourable for gold (Fig. 32).

Geological observation

The visited area was characterised by small and large enclaves of grey homogenous fine-grained amphibolite of variable sizes (probably up to tens of metres) infiltrated by abundant granitic-pegmatitic veins which in places produce an agmatitic rock. Epidotised amphibolite is also encountered. The gneisses in the area consist of a mixture of medium-grained dioritic gneiss and tonalitic gneiss, both with sign of retrogression from granulite facies in the form of centimetre-sized blebs of actinolitic hornblende and sheaf-like biotite. Post-kinematic diorite is also observed. A pronounced brittle-ductile fault zone (060°/c. 55°SE) with chloritised K-feldspar-epidot-mica-quartz impregnated country rocks was encountered in the area. This zone is also infiltrated by abundant quartz/granitic veins.

Geochemistry

Despite a general enrichment in La, and for one sample also enrichment in Na_2O, is observed from the lithogeochemistry of collected rock samples from the landing site in the outer Fiskefjord, it is in general not possible to make a verification of a data signature similar to that of the Isua group. This group is characterised by high values of Au, Cs, La, MgO, Fe_2O, Na_2O and Ni/Mg in stream sediment geochemistry. Collected soil sediment samples from the location have also not been able to make a verification of the data signatures. Nevertheless, some data signatures was verified and enrichment in other elements such as Ce, Sb, Sr, Cu, which in cases are regarded as pathfinder elements for gold, was observed. Furthermore, geological observations such as different granitic-pegmatitic rocks in the area, alteration of amphibolite and alteration in brittle-ductile fault zones makes the area prospective for gold.

Table 13. *Summarised lithogeochemistry of the collected rocks samples from the reconnaissance stop at outer Fiskefjord. The table contains elements found to be indicative for the Isua group (REF) and elements regarded as possible trace elements from gold. Elements regarded as enriched relative to normal values from rocks throughout the Nuuk region are given in red colours; slightly elevated in green. Gold was not encountered in any of the samples.*

Sample no.	Description	As ppm	Ag ppm	Ce ppm	Cr ppm	Cs ppm	Cu ppm	La ppm	Ni ppm	Sb ppm	Sr ppm
482066	Rusty amphibolite w. quartz sweats/veins and disseminated iron-sulphides	<2	<0.5	91	43	<0.5	662	54.3	25	0.3	636
482067	Representative amphibolite – homogenous, relative rich in felsic minerals	<2	<0.5	160	41	<0.5	55	94.5	127	<0.2	599
482069	Altered amphibolite (chlorite-Kfsp.-epidote-qtz.-mica) from central part of brittle-ductile fault zone	<2	<0.5	42	16	<0.5	28	25.2	19	<0.2	1188

Continued		Th ppm	U ppm	W ppm	Zn ppm	Fe_2O_3 %	Na %	Ni/Mg	Ni+Cr
482066	- see above	5	1.9	<3	80	12.29	2.86	10.44	52
482067	- see above	9.1	2.5	<3	97	11.06	1.93	25.34	411
482069	- see above	<0.5	<0.5	<3	72	5.11	4.57	12.40	44

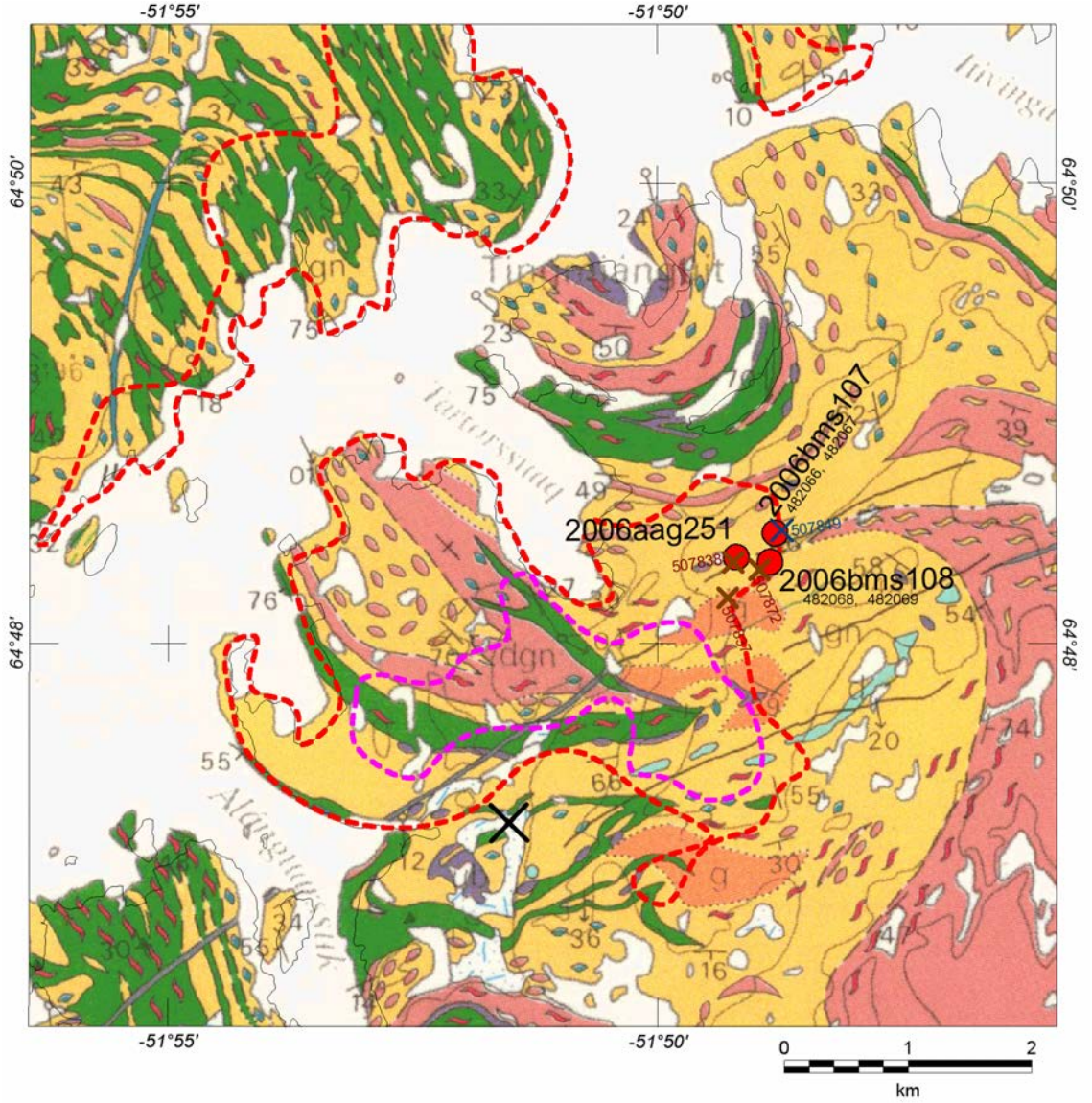

Figure 32. *The location of the reconnaissance stop at the outer part of Fiskefjord. Visited localities with geological observations and samples are indicated by red circles and locality number with rock sample numbers beneath. Soil sediment samples are indicated by brown crosses, while stream sediment samples are indicated by blues crosses. The geological map is a scanned georeferenced version of the 1:100 000 scale Fiskefjord map sheet (Garde 1989). Green colours are amphibolite, light green units are leuco-amphibolite, yellowish brown colours are gneisses, dark pinkish colours are mafic dioritic gneiss, orange colours are granite, red colours are pegmatite and purple are ultramafic rock. Misfit between the coast line in black and the geological map is the result of the use of an older topographical base for the geological map. The sample locations from GPS readings are plotted with reference to the WGS84 datum. The dashed red line outlines the 2.5% most favourable area for Isua gold group. The 1% most favourable area is outlined by the dashed pink line.*

SW of Isua – reconnaissance stop B (area 5)

A small area southwest of the Isua greenstone belt is predicted as being part of the most favourable area for data signatures similar to both the Isua and the Bjørneøen gold groups (Figs 34 and 35). No prior information on gold has been reported from this area, but many gold showings in various settings are known from the Isua greenstone belt situated to the northeast.

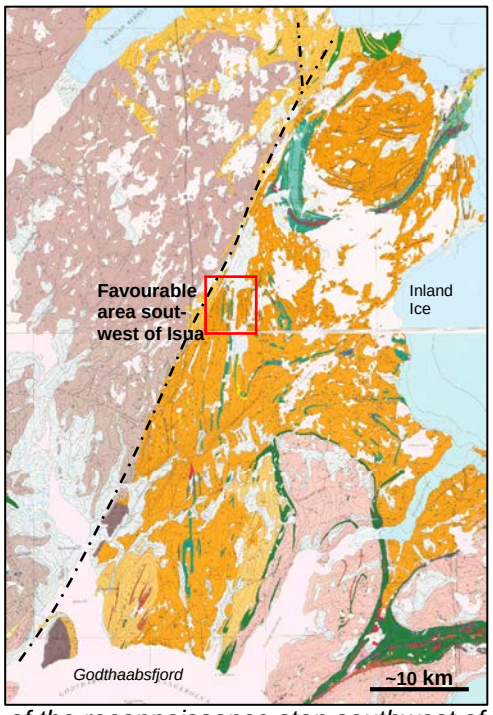

Figure 33. *The location of the reconnaissance stop southwest of Isua greenstone belt is indicated by a red rectangle.*

Geological observations

The visited most favourable area is situated within two 100–300 m wide slivers of supracrustal rocks in gneiss. Notable is also that the area is located 2–3 km away from the main expression of the Ataneq fault zone (which probably also is the continuation of the Ivinnguit fault zone). Several smaller faults, parallel or conjugated to the Ataneq fault cross-cut the visited area (Fig. 34). Much of the ground around the landing site is a block field (Fig. 33) with blocks of grey orthogneiss, supracrustal and siliceous and calcareous, intensely folded blocks.

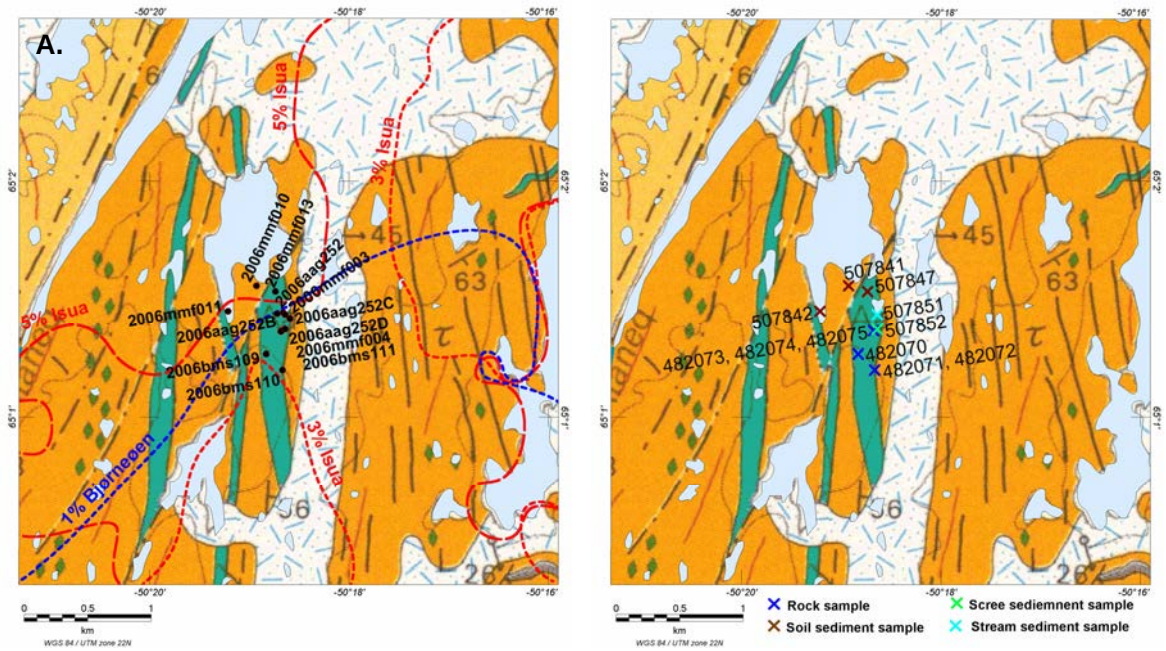

Figure 34. ***A.*** *Outline of the most favourable areas defined from the statistical analysis south-west of Isua together with locations of visited localities (shown by black dots labelled with locality name). Long dashed red lines indicate the outline of the 5% most favourable area for the Isua group, whereas short dashed red lines indicate the 3% most favourable area. The blue short dashed line indicates the outline of the 1% most favourable area for the Bjørneøen group. The labels for the lines are placed outside the favourable areas. The outline of favourable areas for the Isua group is based on the prediction results from Au, Cs, La, MgO, Fe2O, Na2O, Ni+Cr, Ni/Mg from fine fraction stream sediment geochemistry, vertical gradient of total magnetic field intensity and amplitude of the horizontal gradients of total magnetic intensity field from aeromagnetic data, and eU/Th from regional aeroradiometric data. The outline of the favourable area for the Bjørneøen group is based on the distribution of Cs, Rb, U, Th, Mg, Ni+Cr, Ni/Mg in fine fraction stream sediment data. See Stensgaard et al. (2006b) for details on the statistical prediction.* ***B.*** *Distribution of collected rock and sediment samples from the visited area. Geological map: in light green colours are Kailua association supracrustal rocks (mainly amphibolite); dark orange is Early Archaean gneisses (Amitsoq gneiss); light orange is undifferentiated gneiss; black lines indicate the mafic Tarsier dykes (equivalent to the Ameralik dykes south of 65°); black dash-dotted lines indicate faults (with the major Ataneq fault in the left corner of the map).*

Figure 35. *Visited area southwest of Isua (the Inland Ice at Isua is seen in the background in left part of the picture). The distance from the lake in the foreground to the location with the rusty quartz-layer is c. 500 m. The helicopter is seen in the left side of the picture for scale.*

Outcrops in the area around the landing site (at *c.* 50.31667°W and 65.025°N) comprise mainly migmatised gneisses, amphibolite and ultrabasic rocks (Fig. 35). The rocks are strongly deformed and folded. The amphibolite is fine-grained and finely mm-scale layered (Fig. 36). The amphibolite is furthermore intensely sheared and deformed giving rise to flaggy amphibolite schist. Quartz veins/sweats, up to 10 cm in thickness and up to several metres in length, seem to be folded together with the amphibolite.

Figure 36. *Normal grey fine-grained finely layered folded amphibolite with folded quartz veins/sweats. Hammer for scale (c. 60 cm). Locality no. 2006bms106.*

Just south of the landing site a *c.* 5–7 m wide brownish coloured zone in the amphibolite was discovered (Fig. 37; locality no. 2006bms110). This zone is impregnated with quartz (silicified) and is crosscut by quartz and carbonate veins (the carbonate give is causing the brown colouring). The quartz occurs in some cases together with fuchsite. The zone also comprises a high content of dark mica (biotite). Garnetitic-garnet rich parts/bands, with up to 1 cm large garnets, are also present within the zone.

Figure 37. *Brownish carbonate-quartz veined/impregnated zone with iron-sulphides and garnets. Half hammer shaft for scale (c. 1.5 cm).*

Another interesting zone was discovered close to the landing site. The zone is less than 5 m wide. The host rock is strongly sheared amphibolite, which towards the centre of the zone, is succeeded by a fine-grained siliceous garnet-bearing grey-brown rock with conformable quartz veinlets (Fig. 38; locality no. 2006bms111). Locally, also calc-silicate stringers 1 cm thick were observed. Most of the garnets are strongly elongated, c. 0.1 x 1 cm in size, intensely deformed. The centre of the zone consists of a ≤ 50 cm rusty weathering fuchsite-quartzite layer. Adjacent to the fuchsite-quartzite occur a possible mafic metadyke (?), up to 20 cm wide, which appears unaltered except for a few garnets. It is uncertain if the symmetric sequence is the same which in the literature have been described as the 'Akillia association sedimentary rocks' or if these rocks represents hydrothermally altered amphibolite like the one observed in the Qussuk area (see A.A. Garde in Stendal 2007). In places, the amphibolite contains layering of very fine-grained felsic/mafic components that could be of primary origin but completely transformed by intense altera-

tion. The zone could be a possible extension of the brownish coloured quartz-carbonate veined zone also discovered at the landing site.

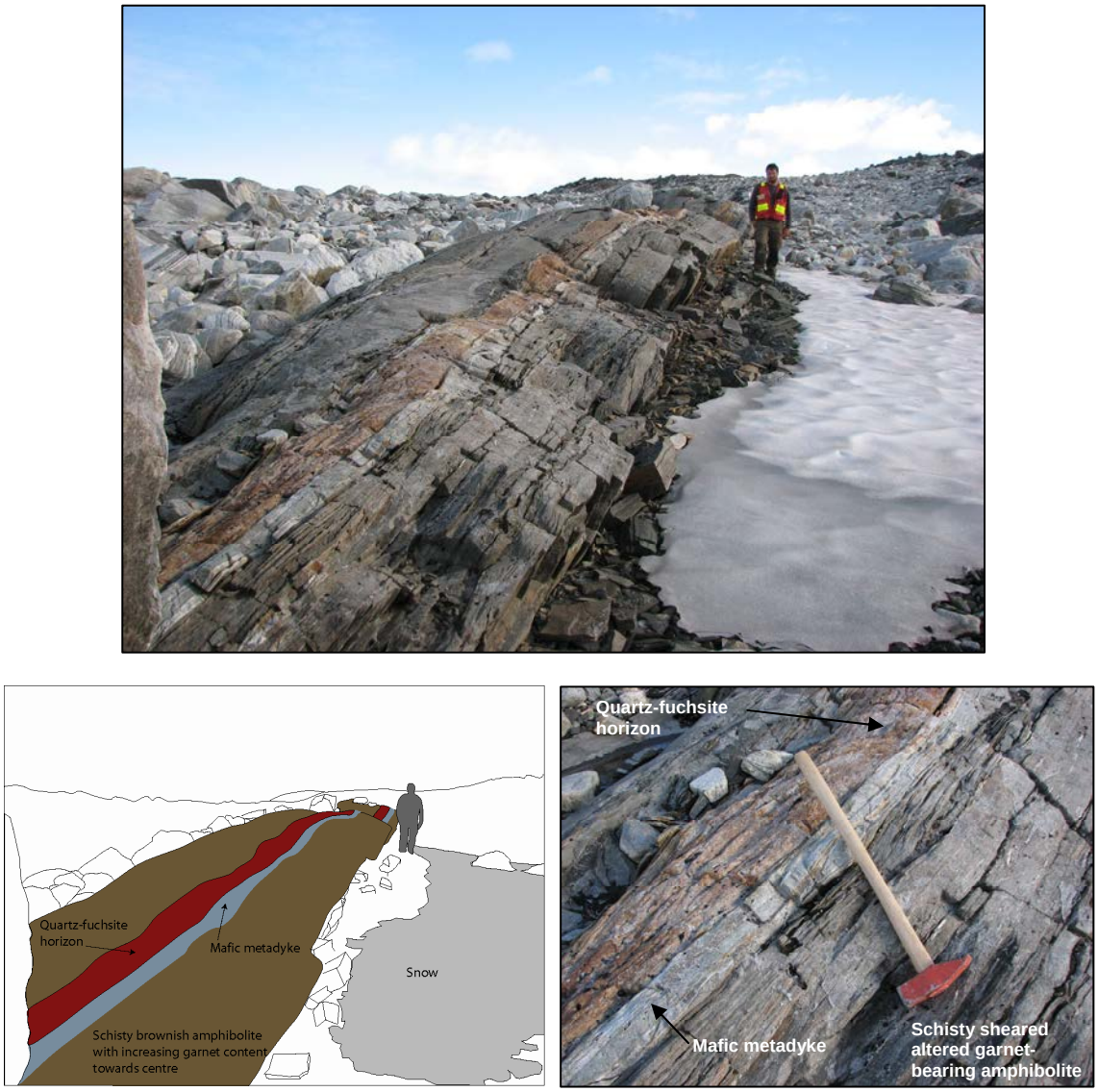

Figure 38. *Zone with sheared garnet-bearing amphibolite and a central quartz-fuchsite layer. A mafic metadyke (?) runs along the western margin of the layer. The uppermost picture is taken towards south. Locality 2006bms111.*

A 50 m wide and *c.* 100 m long body of serpentinised and intensely carbonate-veined and -patched ultrabasic rock is also found adjacent to the landing site (Fig. 35). The body appears to be only little deformed internally, but has a peculiar, centimetre-scale carbonate-spotted texture. It seems that the ultrabasic body is located at/in the eastern margin of the amphibolite sliver, with gneisses towards the east.

Geochemistry

Selected geochemical results of collected rock and sediment samples from the reconnaissance stop are given in Table 14 and Table 15. Four rock samples and five sediment samples have been analysed.

Bjørneøen gold group has strongly indicative high content of Cs, Rb, Th, Ni/Mg ratio, MgO and Ni+Cr in the stream sediment geochemistry. La, U, Fe_2O_3, Na_2O, V, Zn, Zr are moderately indicative for this group. For the Isua group is Au, Cs, La, Sb, Ni/Mg-ratio, Ni+Cr, Fe_2O_3, Na_2O found to be strongly indicative, whereas Rb, Zn and Zr are moderately indicative. Other elements in the stream sediment geochemistry, where characteristics of the two groups have been extracted and where no indicative characteristics have been found are: CaO, K_2O, P_2O_5, SiO_2, and TiO_2.

All the above indicative elements have also been found to be enriched in one or more analysed rock samples or sediment samples from the area.

Most significant for gold content is a soil sediment sample (sample no. 507842) running 158 ppb Au and 701 ppm As together with high values in Cs, Rb and slightly elevated values in Pb, Fe_2O_3 and K_2O. The high Au and As content is not followed by high S content, which was to be expected if sulphides had been present. However, this may simply be a result of breakdown and washout of sulphur in the soil. If is worthwhile noticing, that this sample represents a soil sample of local material below a rusty band/lens in the amphibolite.

A representative non-mineralised amphibolite rock sample (sample no 482070) from the area yields enrichments in Ba (1420 ppm), Ce (193 ppm), La (117 ppm), Sr (1062 ppm) and Th (7 ppm). Slightly elevated content is also observed in U, CaO and MgO. Rock samples from the carbonate-quartz veined/impregnated brown garnet- and iron-sulphide-bearing amphibolite zone (sample nos 482071 and -72) yields enrichment in Cs, Rb, Sb, Fe_2O_3 and K_2O together with slightly elevated values in Ba. Slightly raised Au content of 11 ppm Au is also encountered in one of the samples from this zone (sample no. 482071). This is only regarded as just above the normal background values for amphibolites; but indicates that gold is present in the area.

Cs, Rb and K_2O are found to be enriched and/or slightly elevated in almost all samples from the area. No significant values are obtained in Ni+Cr, Zn, Zr or Ni/Mg ratio which from the statistical extraction were found to be indicative of the Bjørneøen and Isua gold group.

In general, the obtained geochemical results verify the favourability for gold in the area. Overall the relative high content in the alkali metals K_2O, CaO, Rb, Sr, Cs, and Ba, together with high content in the lanthanoids La and Ce and the geological observations indicate that the area possible has been affected by intense hydrothermal activity and the high content of elements regarded as pathfinder for gold such as Au, As, Sb, Cs are also intriguing. As no of the analysed rock samples from the area have contained highly increased gold or arsenic content is the exact rock source rock for these probably not discovered yet.

Table 14. *Geochemistry of collected rock and sediment samples from reconnaissance stop southwest of Isua. Only elements found to be indicative for the Bjørneøen and Isua gold groups and other elements regarded as possible pathfinder elements for gold mineralisations are given. Enriched values are in red; elevated in blue. SSL, soil sediment sample; SSC, scree sediment sample; SSS, stream sediment sample; na, not available/analysed.*

Sample	Locality	Type	Description	Au	As	Ba	Ce	Cr	Cs	Cu	La	Ni	Pb	Rb	Sb	Sr
				ppb	ppm	ppm	ppm	ppm	ppm	ppm	ppm.	ppm	ppm	ppm	ppm	ppm
482070	2006bms109	Rock	Representative sample of fine-grained mafic amphibolite, strongly deformed and sheared - in parts almost with schistosity.	<5	<2	1430	193	32	<0.5	13	117	54	14	50	<0.2	1062
482071	2006bms110	Rock	Sample of brownish 2–3 m wide zone of "straight" amphibolitic mafic schist (deformed/sheared) with disseminated sulphides and qtz-carbonate veins and increased biotite-content - qtz impregnated. Some of the qtz-carbonate veins are up to 10–15 cm thick and may contain fuchsite. Small (<1 mm) disseminated sulphide grains are obs in the zone. The zone has also parts/bands of up to 1 cm garnets.	11	<2	509	23	32	24.9	252	14.2	68	11	160	0.4	161
482072	2006bms110	Rock	Sample of carbonate-qtz veins with fuchsite. From brownish 2–3 m wide zone of "straight" amphibolitic mafic schist (deformed/sheared) with disseminated sulphides and qtz-carbonate veins and increased biotite-content - qtz impregnated. Some of the qtz-carbonate veins are up to 10–15 cm thick and may contain fuchsite. Small (<1 mm) disseminated sulphide grains are obs in the zone. The zone has also parts/bands of up to 1 cm garnets.	<5	2	630	15	84	12.6	128	5.8	66	18	60	0.5	63
482074	2006bms111	Rock	Garnet-bearing amphibolite with qtz veins and disseminated sulphides.	<5	<2	345	14	333	5.8	78	5.4	50	20	70	<0.5	111
507841	2006nmf010	SSL	SSL from boulder-field.	<2	<0.5	230	42	239	3	46	28.4	141	26	67	<0.1	309
507842	2006nmf011	SSL	SSL beneath rusty lens/band. Local material, no cover.	154	701.0	320	39	140	7	243	24.3	117	55	101	<0.1	297
507847	2006nmf013	SSL/ SSS	SSL taken between icefane and a small lake. Blocks of gneiss, amphibolite, gabbro.	<2	<0.5	440	29	259	5	31	17.6	93	18	68	<0.1	269
507851	2006nmf003	SSS	SSS from local small stream running between larger boulders and blocks.	2	<0.5	480	35	134	2	23	19.6	66	21	70	<0.1	340
507852	2006nmf004	SSC	SSC from local hill - ultramafic rocks with rusty layers, talc and serpentinite.	<2	<0.5	320	40	219	2	28	20.5	102	17	<15	<0.1	312

Table 15. *Geochemistry of collected rock and sediment samples from reconnaissance stop southwest of Isua (continuation of Table 14). See former table for explanation of the table.*

Sample	Locality	Type	Description	Zn	Zr	CaO	Th	U	U/Th	Fe_2O_3	K_2O	MgO	Na_2O	S	Ni+Cr	Ni/Mg
				ppm	ppm	pct.	ppm	ppm	ratio	pct.	pct.	pct.	pct.	pct.	ppm	ratio
482070	2006bms109	Rock	Representative sample of fine-grained mafic amphibolite, strongly deformed and sheared - in parts almost with schistosity.	97	67	11.72	7.62	1.32	0.17	12.07	1.04	8.98	0.41	0.03	86	9.97
482071	2006bms110	Rock	Sample of brownish 2–3 m wide zone of "straight" amphibolitic mafic schist (deformed/sheared) with disseminated sulphides and qtz-carbonate veins and increased biotite-content - qtz impregnated. Some of the qtz-carbonate veins are up to 10–15 cm thick and may contain fuchsite. Small (<1 mm) disseminated sulphide grains are obs in the zone. The zone has also parts/bands of up to 1 cm garnets.	85	105	2.58	2.75	0.57	0.20	8.12	3.6	3.85	2.38	0.02	100	29.28
482072	2006bms110	Rock	Sample of carbonate-qtz veins with fuchsite. From brownish 2–3 m wide zone of "straight" amphibolitic mafic schist (deformed/sheared) with disseminated sulphides and qtz-carbonate veins and increased biotite-content - qtz impregnated. Some of the qtz-carbonate veins are up to 10-15 cm thick and may contain fuchsite. Small (<1 mm) disseminated sulphide grains are obs in the zone. The zone has also parts/bands of up to 1 cm garnets.	168	101	4.73	1.16	0.26	0.22	15.34	1.41	5.02	2.17	0.24	150	21.80
482074	2006bms111	Rock	Garnet-bearing amphibolite with qtz veins and disseminated sulphides.	78	50	6.03	0.61	0.17	0.27	8.62	1.42	4.66	4	0.14	383	17.79
507841	2006mmf010	SSL	SSL from boulder-field.	74	na	4.70	3.3	1.5	0.45	6.23	1.90	8.83	2.97	<0.01	380	58.3
507842	2006mmf011	SSL	SSL beneath rusty lens/band. Local material, no cover.	89	na	5.26	2.4	1.8	0.75	10.22	2.05	8.65	2.33	0.02	257	49.4
507847	2006mmf013	SSL/ SSS	SSL taken between icefane and a small lake. Blocks of gneiss, amphibolite, gabbro.	48	na	3.88	3.5	1.4	0.4	4.62	1.80	5.95	3.09	0.01	352	57.0
507851	2006mmf003	SSS	SSS from local small stream running between larger boulders and blocks.	48	na	4.92	3.8	<0.5	na	4.19	2	4.74	3.65	0.01	200	50.1
507852	2006mmf004	SSC	SSC from local hill - ultramafic rocks with rusty layers, talc and serpentinite.	50	na	4.62	3.9	2.3	0.59	5.13	1.67	5.87	3.52	0.01	321	63.4

North of the glacier Sarqap Sermia – reconnaissance stop C (area 6)

Prediction results for the Isua gold group delineate several areas north of the glacier Sarqap Sermia as being part of the most favourable area for this group. The landing site lies at the margin of one of the largest predicted areas within a kilometre-sized amphibolite unit (Fig. 39). Complexes of gneisses and intricately folded amphibolite units and associated large bodies of ultrabasic rocks dominate this region. (Allaart *et al.* 1982).

Geological observations

The amphibolite is fine-grained, mafic, normal amphibolite s.s. with calc-silicates (diopside-plagioclase-garnet) as lenses and strings up to a few centimetres. Few thin quartz veins parallel to foliation is observed. Weak deformed lensoid structures in the amphibolite may represents relict pillow structures.

Geochemistry

A verification of the data signatures of the Isua group can not be made from the geochemical results of the analysed samples from the area (Table 16) and no notable values arise, though a stream sediment samples yields enrichment in As (10.2 ppm) and Cr (443 ppm) together with slightly elevated values in Ni (255 ppm).

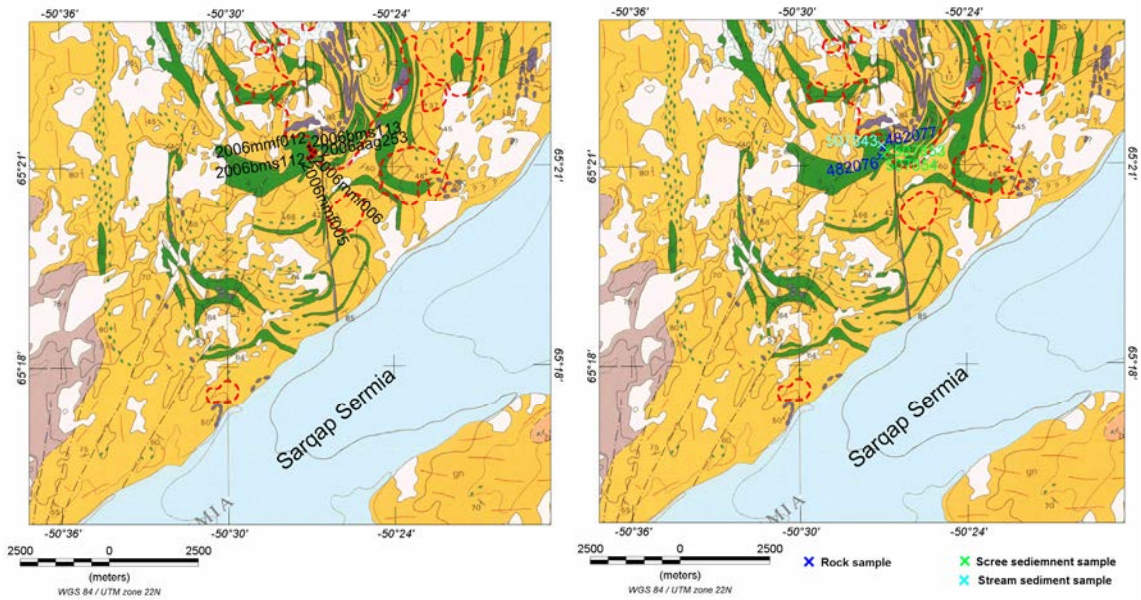

Figure 39. *Maps showing the location of the visitted area north of the glacier Sarqap Sermia that were predicted as being favourable for the Isua gold group. The 3% most favourable area for the Isua group is delineated by dashed red lines. The outline of favourable areas for the Isua group is based on the prediction results from Au, Cs, La, MgO, Fe2O, Na2O, Ni+Cr, Ni/Mg ratio from fine fraction stream sediment geochemistry, vertical gradient of total magnetic field intensity and amplitude of the horizontal gradients of total magnetic intensity field from aeromagnetic data, and U/Th ratio from regional aeroradiometric data.*

TTable 16. *Geochemistry of collected rock and sediment samples from reconnaissance stop north of the glacier Sarqap Sermia. Only elements found to be indicative for the Bjørneøen and Isua gold groups and other elements regarded as possible pathfinder elements for gold mineralisations are given. Enriched values are in red; elevated in blue. SC, scree sediment sample; SSS, stream sediment sample; na, not available/analysed.*

Sample	Locality	Type	Description	Au	As	Ba	Ce	Cr	Cs	Cu	La	Ni	Pb	Rb	Sb	Sr
				ppb	ppm	ppm	ppm	ppm	ppm	ppm	ppm.	ppm	ppm	ppm	ppm	ppm
482076	2006bms112	Rock	Representative sample of fine-grained normal dark banded amphibolite. Deformed pillow-structures and calc-silicate alteration is observed.	<5	2	58	18	193	0.7	521	10.9	200	9	<20	<0.2	26
482076	2006bms113	Rock	Similar to 482076 (above) – but another locality.	<5	<2	38	5	235	<0.5	18	2.2	130	6	<20	<0.2	139
507843	2006mmf012	SSS	From dry stream.	<2	10,2	260	32	443	<1.0	60	15.7	255	12	<15	<0.1	338
507853	2006mmf005	SSL	Scree below amphibolite.	<2	2.5	310	43	213	2.0	395	17.0	220	27	35	<0.1	254
507854	2006mmf006	SSL	Scree below amphibolite.	<2	<0.5	<50	20	101	<1.0	357	10.5	97	8	<15	<0.1	254
Sample	Locality	Type	Description	Zn	Zr	CaO	Th	U	U/Th	Fe_2O_3	K_2O	MgO	Na_2O	S	Ni+Cr	Ni/Mg
				ppm	ppm	pct.	ppm	ppm	ratio	pct.	pct.	pct.	pct.	pct.	ppm	ratio
482076	2006bms112	Rock	- continued - see above	339	94	7.19	2.5	0.7	0.28	17.78	0.28	6.44	1.22	1	393	51.5
482076	2006bms113	Rock	- continued - see above	79	39	12.46	<0.5	<0.5	Na	13.41	0.19	8.35	1.51	0.02	365	25.8
507843	2006mmf012	SSS	- continued - see above	57	na	5.40	2.8	<0.5	na	6.98	1.28	12.18	2.98	0.02	698	76.4
507853	2006mmf005	SSL	- continued - see above	85	na	6.80	2.9	<0.5	na	10.42	1.65	9.56	2.94	0.04	433	84.0
507854	2006mmf006	SSL	- continued - see above	74	na	7.47	1.9	<0.5	na	12.13	0.96	8.68	3.14	0.03	198	40.8

Discussion

Signatures of visit areas in relation to established signatures of gold showings

As pointed out in Stensgaard (2006b) is it not likely that the analysed regional datasets can be used to exactly pin-point a small target such as a gold showing. However, the statistical classification of data signatures for areas with known gold occurrences enable the identification of areas with similar data signatures as for the gold showings. Thus, the analyses are more directed towards identification of areas with environments favourable for gold than the gold occurrences themselves.

The ability to statistical identify areas with data signature similar to those with known gold occurrences in the Nuuk region has been verified though the fieldwork. In all visited areas were sought-for characteristics recognised from geological observation and/or rock or sediment geochemistry. The numbers of positive recognised characteristics varies. In some areas were almost all characteristics recognised, whereas only a few characteristics were recognised in others.

The known gold showings used as input in the statistical analysis are all located within supracrustal sequences dominated by metavolcanic rocks, which implied that areas with geochemical signatures of these rocks (e.g. high Mg, Ni and Cr) would be identified. This is also the case; such signature has been confirmed from the favourable areas visited during fieldwork and the favourable areas are within/adjacent to supracrustal units. However, several other data signatures, which not necessarily can be related to the primary environment, have also been identified. Based on the fieldwork it is found, that these signatures probably can be related to introduction of other rock types after the formation of the primary environment, alteration and/or mineralisation processes. It is also notable, that an enrichment in gold itself together with geochemical pathfinder elements for gold, which from the regional stream sediment data was not identified as a part of the data signatures for the favourable areas have been encountered in a couple of the visited areas.

Ni/Mg

Favourable areas are limited to areas with supracrustal rocks, many supracrustal rock units are not outlined as favourable. This implies, that the outlined favourable areas within or near mapped supracrustal units differs from non-predicted areas with supracrustal units. One of the most notable characteristics for the predicted favourable areas with known gold showings is a high Ni/Mg ratio in stream sediment geochemistry.

An investigation of existing lithogeochemical data from the Nuuk region was reported in Stensgaard *et al.* (2006b). All analysed and available rock samples collected by GEUS and

BMP projects in the Nuuk region 2003 – 2006 were compiled (Fig. 40) and it confirmed that previously known gold bearing areas (Storø, Bjørneøen, Ivisaartoq and Qussuk) contained rocks with elevated Ni/Mg ratio (see Fig. 46 in Stensgaard *et al.* (2006b)) as well as predicted favourable areas that falls within the extension of the gold bearing areas. From this investigation, a relation between predicted favourable areas and high Ni/Mg in already collected rock samples was verified. However, most of the investigated samples fall within the extension of already known gold bearing areas.

One of the objectives with the fieldwork in 2006 was to test, whether lithogeochemistry from favourable areas outside known gold bearing tracts (e.g., Fiskefjord) would comprise the above-mentioned characteristic.

Ni and Mg for samples from the favourable areas visited in 2006 was plotted together with samples from the previously years (Fig. 41). Twelve 2006 samples plotted in the excess-Ni field. Thus, it has been verified that also rocks from outlined favourable areas outside previously known gold potential areas also contain samples with high Ni/Mg. The 2006 samples with excess of Ni relative to Mg originate from Fiskefjord, Serfarsuit, and the Qooqqut Lake area (Fig. 42).

As discussed in Stensgaard *et al.* (2006b) the increased Ni/Mg ratio was taken as a sign of alteration and/or mineralisation. Both features were encountered in the 2006 visited favourable areas. That the high Ni/Mg ratio is spatial related to areas with possible gold mineralisation is supported by the encountered elevated gold content in samples from the Fiskefjord area and, though not duplicated during this project, in the Qooqqut area where 200–380 ppb Au content in rock samples previously have been reported by NunaMinerals A/S.

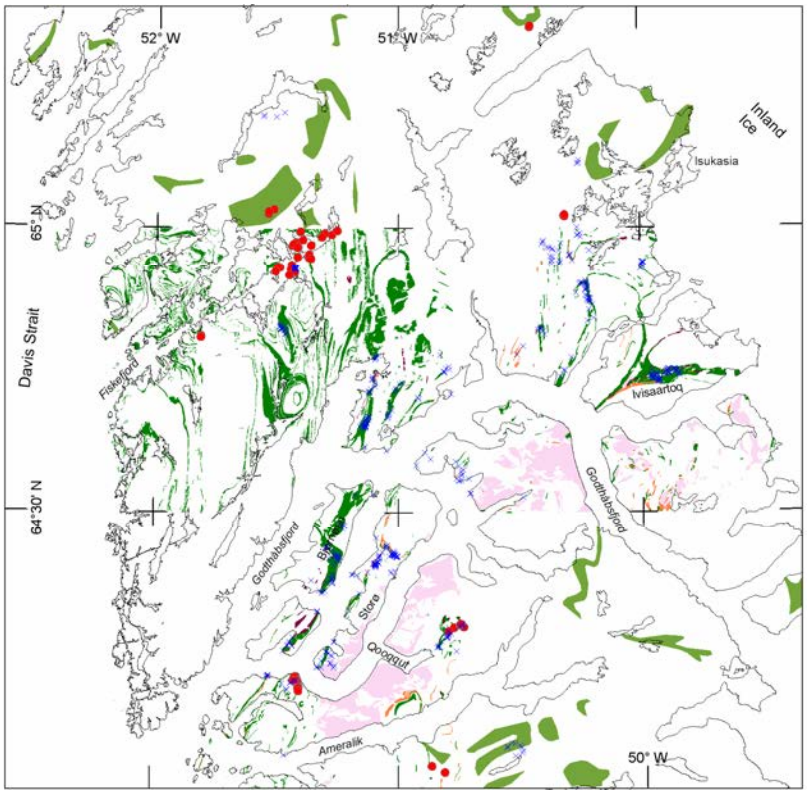

Figure 40. *Simplified geological map with localities of all available and analysed rocks collected by GEUS and BMP projects from 2003 – 2005 is shown with blue crosses. Collected and analysed rock samples, collected in 2006 as part of the current project, is shown with red circles. Mapped amphibolite units are shown in light and darker green (from digital version of scale 1: 2 500 000 and 1:100 000 geological maps respectively). Meta-sediment rock units are shown in orange, ultramafic rock units in purple and Qôrqut granite units in pink (the latter three units are all from 1:100 000 scale digital geological maps).*

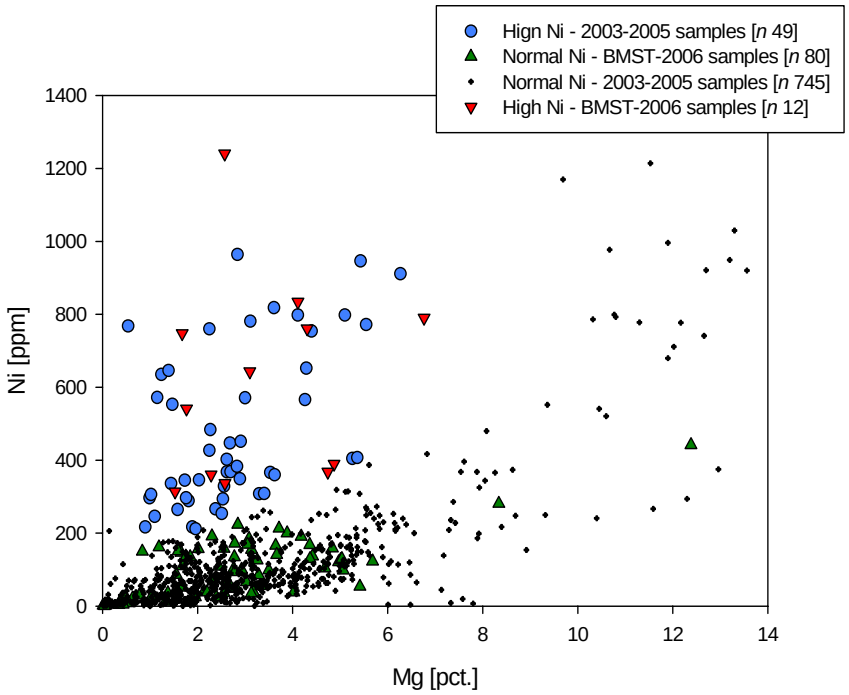

Figure 41. *Plot of Mg vs. Ni. Rock samples with excess of Ni are shown in blue and red.*

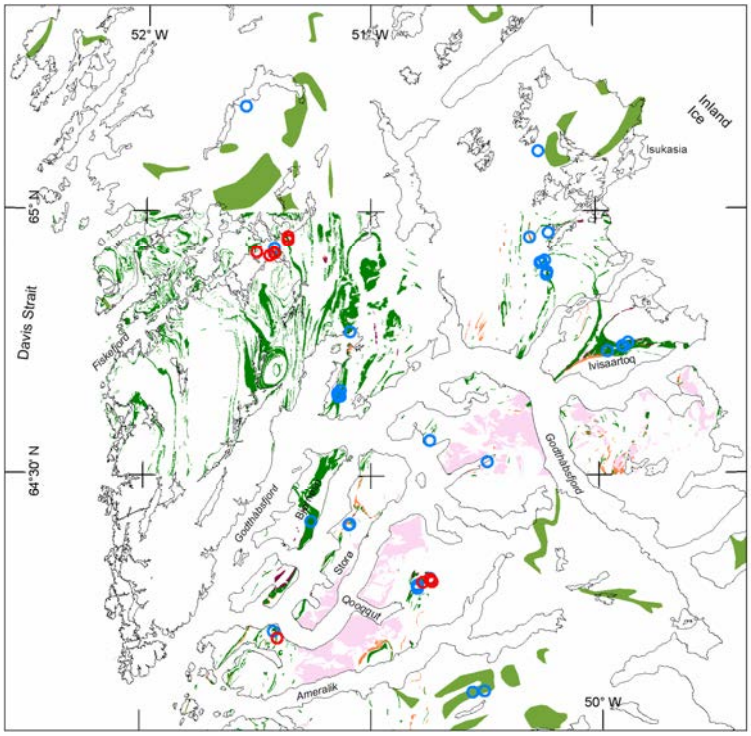

Figure 42. *Simplified geological map with locations of rock samples with excess of Ni relative to Mg. Blue circles arey samples collected from 2003–2005 with excess of Ni, red circles indicates "new" 2006 localities with excess of Ni. Geology as shown in fig. 40.*

Lithological differences between gold hosting areas

As already addressed, all gold hosting and predicted areas are similar in the sense that they are dominated by mafic supracrustal rocks, and have variable proportions of ultramafic rocks and felsic metavolcanic and metasedimentary rocks in the supracrustal packages. Based on the fieldwork in 2006 the table with an overview of similarities and differences between the predicted areas (Stensgaard *et al.* 2006b) has been updated and modified (Table 17).

Table 17. *Overview of lithology and alteration observed in areas with gold showings (Isua, Bjørneøen, and Storø) and predicted gold-favourable areas within the Nuuk region. Up-dated and modified version of table 6 in Stensgaard et al. (2006b)*

Dominating environment:	Accretional		?	xx			×		×						
	Magmatic				xx	×							×	x?	
	Continental		?	x?											
	Island arc			x?				xx							
	Ocean floor	xx	xx	x?	×	×	×		×	xx	xx	xx	×	x?	×
Structures:	Proximal to large tectonic feature	(x)	xx	xx	xx		×						xx	xx	
Alteration:	Massive sulphide		×	×	×	×	×	×	×			×			
	Carbonate veining	×		×						?	?	?		×	
	Quartz veining	×	×	×	×	×	×			×	×	×		×	
	Arsenic present	(x)		×	(x)						(x)			×	
	Seritization	?	?	xx	?			×							
	Silicification	×	(x)	xx	×	×		×							
	Garnetisation			×		×		×	×	×				×	
	Epidotisation	×	×	×	xx		×	×	×			×			
Lithology:	Lamprophyre				×										
	Anorthosite			×											
	Pegmatites		×	xx	xx	×	×		×	×	×		×		
	Iron formation			×											
	Ultrabasic	xx	xx	(x)	xx	×	xx	(x)		×	(x)	xx		×	xx
	Metasediment		×	×				×		(x)					
	Andesite		×	×			×								
	Basalt	×	×	×	×	×	×	×	×	×	×			×	
Gold present:		xx	×	xx	×	(x?)	(x?)	xx				(x)		xx	
		Isua	**Bjørneøen**	**Storø**	**Inner Fiskefjord** (area 1 in this report)	**Qooqqut** (area 2 in this report)	**Sermitsiaq**	**Qussuk**	**Serfarsuit** (area 3 in this report)	**Ujarassauit North**	**Ujarassauit South**	**Ivisaartoq**	**Outer Fiskefjord** (area 4 in this report)	**SW of Isua Greenstone belt** (area 5 in this report)	**North of Sarqap Sermia'** (area 6 in this report)

Summary and concluding remarks

A statistical (e.g., statistical cross-validation, see Stensgaard *et al.* 2006b) and geological (e.g., follow-up on results by fieldwork) verification of the multivariate statistical extraction of data signatures and delineation of areas with similar signature has been attempted during the work in 2006 and 2007; with the results of the fieldwork in 2006 being essential.

Based on the geochemical results attained from the fieldwork it has not always been possible to make a clear verification of signatures similar to that established for the gold groups; in several cases shows only a few of the variables data response similar to those defined for the gold groups. However, when dealing with empirical relations reflecting properties of complex and varying natural phenomena (gold mineralisation) and statistical integrated multivariate responses of processed data which is of relative low resolution compared to the phenomena (gold occurrences) a certain degree of “failure” and uncertainty is expected.

The above results exemplified and emphasises that the results always should be critical reviewed and tested both statistical and geological.

Nevertheless, a clear verification, with positive identification of data signatures and a potential for gold, with rock samples strongly enriched in gold being the final prove, could be established for several areas delineated as favourable for gold (e.g., the area in the inner Fiskefjord and the area south-west of Isua greenstone belt). Geological observations and enrichment in geochemical elements regarded as pathfinder for gold also support a potential in these areas for gold mineralisation.

The verification from the fieldwork and geochemical results together with recommendations on future work is summarised in Table 18.

Table 18. *Summary of results and recommendations for the areas visited during the 2006 fieldwork.*

Area	Result	Recommendation	Resources	Priority
Inner Fiskefjord (area 1)	**Positive.** The geological settings are interesting for mineralisation, a large-scale alteration system along the Fiskefjord fault has been identified and a general enrichment in gold and pathfinder elements has been found. A rather large lithodiversity is observed.	**Follow-up is recommended.** Detailed geological mapping and sampling of supracrustal rock units should be undertaken. Furthermore should a detailed sediment-sampling program over the supracrustal units be undertaken (especially the unit with the highest gold content on the north side of the central part of Fiskefjord).	**Detailed program:** 2 x 2 person team, 2–3 weeks. 3 camps for each team, c 15–20 hours helicopter, use of dinghy analysed of c. 400 samples	**1**
Qooqqut Lake (area 2)	**Negative/Positive.** Similar supracrustal rocks as the once on Storø, high degree of mineralisation but analysed 2006 samples yielded no gold. However earlier work by NunaOil A/S has identified gold in the area and zinc-copper mineralisation were discovered during the fieldwork in 2006.	**Presently no future follow-up for gold.** However, the **zinc showing** is probably too small to be economical, but should perhaps be checked during a short campaign.	Zink showing: 1 x 2 person team, 1 camp, 4–5 days, 4 helicopter hours, 100 samples.	4
Serfarsuit (area 3)	**Negative.** Similar rocks as the once at Storø, however, the proportions of the metasediments and alterations are much smaller.	**No follow-up.**	–	–
Outer Fiskefjord (area 4)	**More follow-up needed; negative results from 2006, but still not fully investigated.** The geological settings are interesting, a large lithodiversity is observed and pronounced alteration systems are identified. No gold in collected samples, however, the reconnaissance stop was outside major supracrustal rock units and the results from the inner part of the Fiskefjord are intriguing for the outer part. Furthermore, several large favourable areas are outlined in the outer part of Fiskefjord and more time is needed to do a full follow-up in this area.	**Follow-up should possible be undertaken**, either as more reconnaissance stops or as a larger program in the area with detailed geological mapping and sampling of supracrustal rock units should be undertaken. Furthermore should a detailed soil sediment sampling program over the supracrustal units be undertaken	**Reconnaissance:** 8 hours of helicopter time, 2–4 persons, 2–4 days. **Alternatively, detailed follow-up:** One team, 3–4 weeks, 3–4 camps, 8 hours of helicopter, use of dinghy.	**3**
SW of Isua greenstone belt (area 5)	**Positive.** Geological settings are interesting, structures intriguing, large-scale alteration systems are observed, and the area is a continuation of the gold bearing Isua greenstone belt. Geochemical results have been very positive; enrichments of gold and arsenic (701 ppm As in sediment!) content together with enrichment/elevated content in other pathfinder elements. On the downside is the size of the supracrustal units – however, the exact size of the units is not fully investigated and the units continue along strike.	**Follow-up is recommended.** The obtained geochemical anomalies and geological settings justify a follow-up – which probably could be very effective due to the probably limited size of the supracrustal units. Detailed geological mapping and sampling of supracrustal rock units should be undertaken. Furthermore should a detailed sediment sampling program over the supracrustal units be undertaken	**Detailed follow-up:** 1–2 x 2 person teams, 2–3 weeks, 3 camps, 15 hours of helicopter, analyses of 250–300 samples.	**2**
North of Sarqap Sermia (area 6)	**Negative – but not fully investigated.** Despite the area host an interesting rock assemblage and rather large proportions of supracrustal the area is scarcely mapped and relatively unknown.	**Presently no further follow-up.** This area and the area to the north comprise some of the largest supracrustal units between Nuuk and Kangerlussuaq. If possibly, these should be investigated in more detail.	–	–

Fieldwork has successfully been carried out in areas predicted as favourable for gold showings from an integrated multivariate statistical analysis of data from the Nuuk region, southern West Greenland.

Six areas where visited. These represents a diversity in possible primary environment; ranging from environments dominated by the magmatic part of an ocean floor environment, the extrusive ocean floor/sedimentary environment, to island arc environment. Characteristic signatures as well as geological observations from the visited areas have been presented. Based on the fieldwork and earlier results of the project an overview of similarities and differences of the known gold bearing areas and the predicted favourable areas has been established.

It was possible to verify a gold potential in two areas, whereas a potential in the others is unsure and not verified; though some characteristics, both geological and geochemical, are similar to those defined for known gold occurrences in the Nuuk region.

The two verified areas with gold potential are the located in the inner part of Fiskefjord and in the area southwest of the Isua greenstone belt. The areas have not prior been explored for gold and no elevated gold content have been reported from these areas. Both geological setting and geochemical results, with elevated gold content and enrichment in pathfinder elements for gold, verifies that these areas have a potential for gold occurrences and that more detailed work should be carried out in these areas.

References

Allaart, J.H. 1982: Geological map of Greenland, 1:500 000, Frederikshåb Isblink - Søndre Strømfjord, sheet 2. Copenhagen: Geological Survey of Greenland.

Allaart, J.H., Hall, R.P., Jensen, S.B. & Stecher, O. 1982: Mapping in the Isukasia area. Rapport Grønlands Geologiske Undersøgelse **110**, 44–45.

Appel, P.W.U., Bliss, I.C., Coller, D.W., Grahl-Madsen, L. & Petersen, J.S. 2000: Recent gold discoveries in Arhaean rocks on central West Greenland. Trans. Instn. Metall. (Sect. B: Applied. Earth Science.) **109**, B34–B41.

Appel, P.W.U., Coller, D., Coller, V., Heijlen, W., Moberg, E., Polat, A., Raith, J., Schjøth, F., Stendal, H. & Thomassen, B. 2005: Is there a gold province in the Nuuk region? Danmarks og Grønlands Geologiske Undersøgelse Rapport **2005/27**, 79 pp., 1 CD-Rom.

Chadwick, B. & Coe, K. 1988: Geological map of Greenland, 1:100 000, Ivisârtoq 64 V.2 Nord. Copenhagen: Geological Survey of Greenland.

Escher, J.C. & Pulvertaft, T.C.R. 1995: Geological map of Greenland, 1:2 500 000. Copenhagen, Denmark: Geological Survey of Greenland.

Friend, C.R.L. & Nutman, A.P. 2005: New pieces to the Archaean terrane jigsaw puzzle in the Nuuk region, southern West Greenland: steps in transforming a simple insight into a complex regional tectonothermal model. Journal Geological Society, London **162**, 147–162.

Garde, A.A. 1989: Geological map of Greenland, 1:100 000, Fiskefjord 64 V.1 Nord. Copenhagen: Geological Survey of Greenland.

Garde, A.A. 1997: Accretion and evolution of an Archaean high-grade grey gneiss - amphibolite complex: the Fiskefjord area, soutehrn West Greenland. Geology of Greenland Survey Bulletin **177**, 115 pp.

Garde, A.A. 2007: A mid-Archaean island arc complex in the eastern Akia terrane, Godthåbsfjord, southern West Greenland. Journal of the Geological Society, **164**, 565–579.

Garde, A.A., Stendal, H. & Stensgaard, B.M. 2007: Pre-metamorphic hydrothermal alteration with gold in a mid-Archaean island arc, Godthåbsfjord, West Greenland. Geology Survey of Denmark and Greenland Bulletin **13**, 37–40.

Hollis, J.A. 2005: Greenstone belts in the central Godthåbsfjord region, southern West Greenland. Geochemistry, geochronlogy and petrography arising from 2004 field

work, and digital map data: Danmarks og Grønlands Geologiske Undersøgelse Rapport. **2005/42**, 213 pp., 1 DVD.

Hollis, J.A., Frei, D., van Gool, J.A.M., Garde, A.A. & Persson, M. 2006a: Using zircon geochronology to resolve the Archaean geology of southern West Greenland. Geology Survey of Denmark and Greenland Bulletin. Review of Survey Activities 2005. **10**, 49–52.

Hollis, J.A., Garde, A.A., Frei, D. & van Gool, J. 2005: Geochronology. In: Hollis, J.A. (ed.): Greenstone belts in the central Godthåbsfjord region, southern West Greenland. Geochemistry, geochronlogy and petrography arising from 2004 field work, and digital map data **2005/42**, 12–79.

Hollis, J.A., Schmid, S., Stendal, H., van Gool, J.A.M. & Weng, W.L. 2006b: Supracrustal belts in Godthåbsfjord region, southern West Greenland. Progress report on 2005 field work: geological mapping, regional hydrothermal alteration and tectonic sections. Danmarks og Grønlands Geologiske Undersøgelse Rapport **2006/7**, 171 pp., 1 DVD.

Hollis, J.A., van Gool, J.A.M., Steenfelt, A. & Garde, A.A. 2004: Greenstone belts in the central Godthåbsfjord region, southern West Greenland. Preliminary results from field work in 2004. Danmarks og Grønlands Geologiske Undersøgelse Rapport **2004/110**, 110 pp., 1 DVD.

Knudsen, C., van Gool, J.A.M., Østergaard, C., Hollis, J.A., Rink-Jørgensen, M., Persson, M. & Szilas, K. 2007: Gold-hosting supracrustal rocks on Storø, southern West Greenland: lithologies and geological environment. Geology Survey of Denmark and Greenland Bulletin **13**, 41–44.

Jensen, L.S. 1976: A New Cation Plot for Classifying Subalkalic Volcanic Rocks. Ontario Geological Survey Miscellaneous Paper **66**.

Juul-Pedersen, A., Frei, R., Appel, P.W.U., Persson, M. & Konnerup-Madsen, J. 2007: A shear zone related greenstone belt hosted gold mineralization in hte Archean of West Greenland. A petrographic and combined Pb-Pb and Rb-Sr geochronological study. Ore Geology Reviews **32**, 20–36.

McGregor, V.R. 1983: Geological map of Greenland, 1:100 000, Qôrqut 64 V.1 Syd. Copenhagen: Geological Survey of Greenland.

Nakamura, N. 1974: Determination of REE, Ba, Fe, Mg, Na and K in carbonaceous and ordinary chondrites. Geochim Cosmochim Acta **38**, 757–775.

Nielsen, B.M., Rasmussen, T.M. & Steenfelt, A. 2004: Gold potential of the Nuuk region based on multi-parameter spatial modelling of known gold showings. Danmarks og Grønlands Geologiske Undersøgelse Rapport **2004/121**, 155 pp.

Pasi, E., Garofalo, P., Appel, P.W.U. & Heijlen, W. 2006: Alteration patterns in Au-mineralised zones of Storø, Nuuk region - West Greenland. Danmarks og Grønlands Geologiske Undersøgelse Rapport **2006/30**, 73 pp.

Pearce, J.A. & Cann, J.R. 1973: Tectonic setting of basic volcanic rocks determined using trace element analyses Earth and Planetary Science Letters **19**, 290–300.

Persson, M.F. 2007: Metamorphic and geochronological evolution of the Au-bearing rocks on central Storø, Nuuk region, West Greenland, 98. Unpublished Master's Thesis thesis, University of Copenhagen.

Steenfelt, A. 1987: Geochemical mapping and prospecting in Greenland - a review of results and experience. Journal of Geochemical Exploration **29**, 183–205.

Steenfelt, A. 1990: Geochemical patterns related to major tectono-stratigraphic units in the Precambrian of norhtern Scandinavia and Greenland. Journal of Geochemical Exploration **39**, 35–48.

Stendal, H. 2007: Characterisation of selected geological environments. Mineral resource assessment of the Archaean Craton (66° to 63°30') SW Greenland. Contribution no. 1: Danmark og Grønlands Geologiske Undersøgelse Rapport. **2007/20**, 90.

Stensgaard, B.M., Rasmussen, T.M. & Steenfelt, A. 2006a: An integrative and quantitative assessment of the gold potential of the Nuuk region, West Greenland. Geology Survey of Denmark and Greenland Bulletin. Review of Survey Activities 2005. **10**, 37–40.

Stensgaard, B.M., Steenfelt, A. & Rasmussen, T.M. 2006b: Gold potential of the Nuuk region based in multi-parameter spatial modelling. Progress 2005. Danmarks og Grønlands Geologiske Undersøgelse Rapport **2006/27**, 207 pp.

Appendix A.

The following text is a modified version from the explanation of the grouping of gold showings and extraction of characteristic signature presented in Nielsen *et al.* (2004).

Grouping of gold showings

For reasons of simplicity the known gold showings in the Nuuk region were at first treated as one group. In the present phase, the multi-parameter signatures of the showings have been investigated to see if there are statistically significant differences among them to justify that they should be divided into subgroups.

The grouping of the gold showings has been based on their ability to predict other showings within the same group. A prediction map was constructed for each gold showing and its capability to predict the remaining showings was examined. A two-dimensional matrix with numbered showings along the axes displays the result of the examination (Fig. 43). Red fields mark a high probability of the prediction. The rows of the matrix contain showings predicted by the showing of the row; the columns contain showings that predict the showing of the column. Gold showings that are mutually predicted (i.e. are able to predict each other, and show similarities in their prediction of other showings) are grouped.

In contrast, gold showings that predicts, and are predicted by an insignificant number or none of the other showings are considered insufficiently characterised to qualify as input data. These are excluded from further analysis. Likewise, sets of very few mutually predicted showings are also excluded from further analysis.

Considering the resolution of the data and the way characteristic signatures of showings are extracted, it lies implicit in the statistical method that showings lying closely together will be grouped, even though they could host different types of gold mineralisation that locally might have distinct signatures.

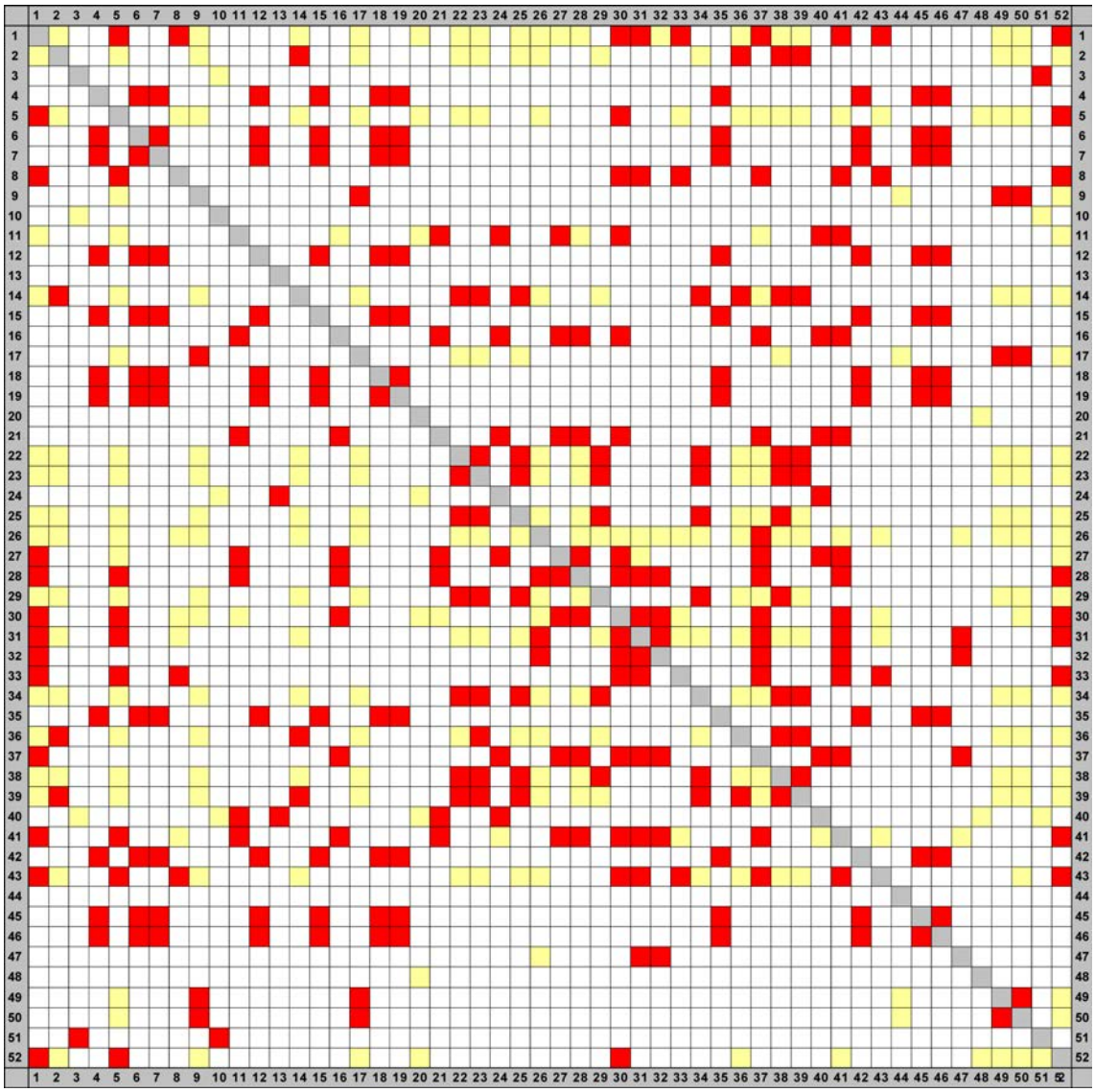

Figure 43. *Prediction matrix illustrating the prediction capabilities of fifty-two gold showings within the Nuuk region. Red squares indicate a prediction probability of above or equal to 99.5%. Yellow squares indicate a prediction probability from 90.0 to 99.4%. Thus, showing no. 18 predicts showings in row 18, i.e. no. 4,6,7,12, 15, 19 etc., and is itself predicted by showings in column 18, i.e. no. 4,6,7, etc. The prediction was based on signatures including As, Au, Ca, Rb, Th, U, and Ni/Mg ratio in stream sediment data, together with the vertical gradient and amplitude of the horizontal gradients of aero-magnetic data. These datasets were found to be indicative of gold showings in the first phase of the project (see Nielsen et al. 2004).*

Groups of gold showings

Based on a visual inspection of the prediction matrix (Fig. 43) three groups of gold showings are identified. Furthermore, one set of showings, the Qangaatarssuakop Isuakasia set, is also identified. This set only contains four showings, which is regarded as statistically insufficient to form a proper group. Consequently, this set of showings is excluded from further analysis in this work. Eight showings are predicted by and predict a very small number of the other showings or none at all. These are also excluded from further analysis. The

members of the identified groups are listed in Table 19 and their spatial distribution is shown in Figure 1. It is noteworthy that the grouping based mainly on geochemistry results in a geographical grouping.

The Isua group contains 19 showings, of which one is located in supracrustal belt at Ivisaartoq, and the remaning within the Isua supracrustal greenstone belt. The Bjørneøen group contains 10 showings all situated within supracrustal belt in the central part of Bjørneøen. The final proper group is the Storø group, which contains 11 showings, all within the supracrustal rocks in the areas at and around the Qingaaq and Aappalaartoq gold prospects.

Table 19. *Identified groups of gold showings. Showing no. refers to the row and column numbers in prediction matrix. The red, blue and green coloured text for three of the groups refers to the colours that are used in other figures to indicate these groups.*

Name of group	Gold showings no.	Number of showings
Isua group	1, 5, 8, 11, 16, 21, 26, 27, 28, 30, 31, 32, 33, 37, 40, 41, 43, 47, 52	19
Bjørneøen group	2, 14, 22, 23, 25, 29, 34, 36, 38, 39	10
Storø group	4, 6, 7, 12, 15, 18, 19, 35, 42, 45, 46	11
Showings excluded from further analysis:		
Qangaatarssuakop Isuakasia set	9, 17, 49, 50	4
No predictions	3, 10, 13, 20, 24, 44, 48, 51	8

Data signatures of the groups

Method for extraction of characteristic data signatures of the gold groups

Empirical distribution functions describe the signature of the gold showings in the available datasets. The determination of the empirical distribution functions is explained in detail in Nielsen *et al.* (2004). For each variable four functions is calculated, one for pixels belonging to each of the three gold showing groups, and one for remaining pixels, defined as the background distribution. Because of the high number of pixels assigned to background compared to the number of pixels assigned to a group the variations of the background signature for different groups will be infinitesimal. The empirical distribution functions are constructed using a smoothed kernel function.

The ratio between the distribution function for a group and for the background – the individual likelihood ratio – can be used to evaluate the significance of the data signature. The ratio ranges from 0 to infinite. To display and discuss the likelihood ratios, they have been normalised using the following function: ratio / (1 + ratio). The normalised ratio range from 0 to 1, and is equal to 0.5, when two distribution functions have the same value. If the empirical likelihood ratio is above 0.7, the data signature can be said to be significant. Examples of data signatures are shown can be seen in Nielsen *et al.* (2004).

Table 20. *All analysed datasets for which signatures of the gold showing groups have been determined.*

Type of data	Datasets	Number of datasets
GEUS fine fraction stream sediment geochemistry	Al_2O_3, As, Au, CaO, Cs, Fe_2O_3 K_2O, La, MgO, Na_2O, Ni+Cr, Ni/Mg ratio, P_2O_5, Rb, Sb, SiO_2, TiO_2, Th, U, V, Zr, Zn	22
GEUS aeromagnetic survey	Total magnetic intensity field (TMI), Vertical gradient of TMI, Amplitude of the horizontal gradients of TMI, Horizontal gradients of TMI (in four directions)	7
GEUS aeroradiometric survey	Total gamma-radiation, K, eTh, eU and eU/eTh ratio	5
Statistically defined lineaments in aeromagnetic data	For search radius 1000m and subdivided into 7 classes according to the length of the lineaments – in total 35 datasets: ❑ Mean direction of lineaments within the search radius ❑ Minimum distance to nearest lineament within the search radius ❑ Number of lineaments crossing the search radius ❑ The total length of the lineaments crossing the search radius ❑ Length of vector sum of unit vectors divided by number of vectors within the search radius – a complexity factor	35
	In total	69

Results

The contoured grids of the GEUS stream sediment geochemistry and the aeromagnetic data are available in Nielsen *et al.* (2004). An overview of all datasets included so far in the project is shown in Table 20. The most significant signatures of the gold showing groups are summarised in Table 21.

GEUS stream sediment geochemistry data

The geochemical signatures for the three groups do not exhibit characteristic contrasts from background in the following chemical components: CaO, K_2O, P_2O_5, Sb, SiO_2, TiO_2, V, Zr, and Zn.

The three groups have high Ni/MgO and high Cs as a common feature, but they are different in the remaining part of their signatures. Medium to high Rb, La, U and Th characterise

the Storø and Bjørneøen groups, while the Isua group has low values in these elements. The Bjørneøen and Isua groups have medium to high MgO, Fe_2O_3, Ni and Cr in common, while the Storø group is characterised by high Al_2O_3. The Isua group has low Na_2O compared to the other groups. Gold in the stream sediment geochemistry is only found to be indicative for the Isua group. Trivial but important observations to keep in mind as high gold values in stream sediment geochemistry only relatively seldom are encountered. The presently analysed stream sediments do not reflect even the gold prospects at Storø – probably an effect of the data resolution. Arsenic is only found to be indicative for the Storø group.

GEUS aeromagnetic data

Though a modestly significant signature is observed for the Storø group, no really significant signature is obtained for any of the groups in the total magnetic field intensity (TMI). Only the Isua group has a significant signature in the aeromagnetic datasets; characteristic very low and very high values are obtained in the vertical gradient of TMI (VG-TMI) and likewise, very high values are obtained in the amplitude of the horizontal gradients of the TMI (Amp.-HG-TMI). However, these signatures are weakly defined and a considerable portion of the showings within the group falls within the range of the background values.

GEUS aeroradiometric data

Aeroradiometric signatures are found to be indicative, especially for the Storø group. This group shows distinct high values in K, Th, Total gamma, U and U/Th ratio signature, which, for the K, Th, and Total gamma radiation, is different from the signatures of the other groups and the background. Moderate values in U and moderate to high values in the U/Th ratio distribution are found for the Isua group. Showings of the Bjørneøen group are not different from background in the aeroradiometric data.

Statistically defined lineaments defined in GEUS aeromagnetic data

Only datasets produced with a search radius of 1000 m have been analysed during the second phase. An indicative minimum distance between 1600–3000 m to nearest lineament when all lengths of lineaments are considered is found to be characteristics for the Bjørneøen group. When lineament lengths between 4250–23600 m (75–100%) are considered an indicative minimum distance between 2000–3250 m is found for this group. For the Storø group an indicative mean direction between 0–25° is found when lineament lengths between 2450–3100 m (25–50%) are considered. When lineament lengths between 3100–4250 m (50–75%) are considered an indicative mean direction of 30° is established for this group. Several other representations of the statistically defined lineaments yields is found to be moderately indicative.

Table 21 *Schematic presentation of signatures in grid values of geochemical and geophysical parameters for gold showing groups against the background. Low, medium, high, highest refer to values relative to background. A full coloured cell marks where a signature is regarded indicative for the group (the likelihood ratio is above 0.7 to 0.8, preferably well above – see diagrams in Appendix C). A hatched cell refers to a signature, which is found to be moderately indicative. Non-coloured cells are non-indicative. Abbreviations used: TMI, total magnetic field intensity; VG, vertical gradient of TMI; Amp.-HG-TMI, amplitude of horizontal gradients of TMI. Minimum distance refers to the minimum distance to the nearest lineament within the search radius.*

Data	Storø group	Bjørneøen group	Isua group	Background
GEUS stream sediment geochemistry:				
Au	Low (as backg., 0-40 ppb)	Low (as backg., 0 – 40 ppb)	**High (> 60 ppb, bimodal)**	Low (0 – 40 ppb)
As	**High (> 20 ppm)**	Low (as backg., < 4 ppm)	Low (as backg., < 4 ppm)	Low (< 4 ppm)
Cs	**High (3.5 – 5 ppm)**	**High (3.5 – 5 ppm)**	**Highest (wide range, 3 – 6.5 ppm, multimodal)**	Low (< 2.5 ppm)
Rb	**High (40 – 80 ppm)**	**High (40 – 80 ppm)**	**High* (slightly lower than the two other groups, 30 – 70 ppm)**	Low (10 – 50 ppm)
La	**High (50 – 70 ppm)**	**Medium (35 – 55 ppm)**	**Low (30 – 10 ppm)**	Medium (wide range, 15 – 50 ppm)
U	**Highest (>80 ppm)**	**Medium (17 – 35 ppm, bimodal)**	Low (as backg., <15 ppm)	Low (< 15 ppm)
Th	**Highest (12.5 – 20 ppm)**	**High (10 – 15 ppm)**	Low (as backg., <8 ppm)	Low (< 12.5 ppm)
Ni/Mg ratio	**High (ratio 30 – 40)**	**High (ratio 30 – 37)**	**High (ratio 30 – 45)**	Low (wide range, ratio 10 – 35)
MgO	Low (2-3%)	**High (3.5 – 4.0%)**	**Medium – High (rel. wide range, 3.0 –-7.0%, bimodal)**	Low (wide range,1.5 – 4.5%)
Ni+Cr	Low (200 – 400 ppm)	**High (400 – 800 ppm)**	**Medium – High (rel. wide range, 300 – 800 ppm)**	Low (150 – 400 ppm)
Al_2O_3	**Highest (15.5 – 16.5 %)**	Low (as backg., 13.5 – 15.0 %)	Low (as backg., 14.0 – 15.5 %)	Low (wide range, 13.5 – 15.5 %)
Fe_2O_3	Low (as backg., 4 – 6 %)	**Medium (as backg., 6 – 7.5 %)**	**Highest (wide range, 7 – 12.5 %, bimodal)**	Low (wide range, 3 – 9 %)
Na_2O	High (as backg., 3.00 – 3.75 %)	**Medium (2.75 – 3.50 %)**	**Low (2.50 – 3.50 %)**	High (3.00 – 4.75 %)
V	Low (60 – 90 ppm)	**High (85 – 105 ppm)**	**High (70** – 150 ppm, multimodal)	Low – Medium (50 – 100 ppm)
Zn	**High (60 – 90 ppm)**	**High (55 – 85 ppm)**	**High (50 – 110 ppm, bimodal)**	Low – Medium (wide 20 – 100 ppm)
Zr	**Low (200 – 450 ppm)**	**Low (200 – 450 ppm)**	**Low (< 300 ppm)**	Medium – High (wide 150 – 900 ppm)

Figure 44 continued

GEUS aeromagnetic data:

TMI	**Low (-450 – -150 nT)**	Medium (-300 – 0 nT)	High (-400 – 400 nT)	Low (wide range, -400 – 700 nT)
VG-TMI	Medium (-0.2 – 0.2 nT/m)	Medium (-0.2 – 0.2 nT/m)	**Lowest and Highest (-0.5 – -0.25 nT/m and 0.4 to 0.75 nT/m)**	Medium (-0.3 – 0.4 nT/m)
Amp.-HG-TMI	Low (0 – 0.1 nT/m)	Low (0 – 0.1 nT/m)	**Highest (wide range, 0.1 – 1.0 nT/m)**	Low (0 – 0.25 nT/m)

GEUS aeroradiometric data:

K	**High (1.75 – 2.5%)**	Medium (as backg., 0.25 – 1.5%, bimodal)	Medium (slightly lower than main backg., 0.50 – 1.25%)	Medium (0.25 – 2.5%l)
Th	**High (8 – 14 ppm)**	Low (as backg., 1 – 8 ppm, bimodal)	Low (4 – 8 ppm)	Low (1 – 10 ppm)
Total gamma	**High (main 10 – 13 Ur, bimodal)**	Low (as backg., 3 – 7Ur, bimodal)	Low (as backg., 5 – 8 Ur)	Low (1 – 10 Ur)
U	**High (2.5 – 5.5ppm, multimodal)**	Medium (0.5 – 1.5%)	**Medium (1 - 4 ppm, multimodal)**	Low (0 – 3 ppm, main <1.5 ppm)
U/Th ratio	**Medium – High (0.25 – 0.55)**	Medium – Low (0.5 – 0.30)	**Medium – High (0.10 – 0.65, multimodal)**	Low (0.00 – 0.30)

Distance to lineaments derived from aeromagnetic data within a search radius of 1 km:

Minimum distance, all lines	**Medium (1200 – 2300 m)**	**High (1600 – 3000 m)**	Low (0 – 1200 m, as main backg.)	Low (wide, 0 – 3600 m)
Minimum distance, 0 – 25%	Low (1000 – 2200 m)	**Medium** 1st peak at 2000 – 2500 m, 2nd peak at 3000 – 4000 m, bimodal)	Medium – **High (trimodal, significant peak at 2500 m – 3500 m)**	Low – High (0 – 4500 m)
Minimum distance, 75 – 100%	**Medium – High (1250 – 3000 m)**	**High (2000 – 3250 m)**	Low (0 – 1500 m)	Low – High (0 – 3000 m)
Minimum distance, 90 – 100%	**Medium (1500 – 2250 m)**	**Medium (2500 – 3500 m)**	Low – Medium (bimodal, 500 – 1500 m and 3500 – 4500 m)	Low – High (0 – 6000 m)
Mean direction, 25 – 50% lines	**Low (0 – 25°)**	**Low and High (bimodal, significant peak 0 – 35°, 2nd smaller peak 130 – 180°)**	Low and High (bimodal, 10 – 30° and 150 – 180°)	Low – High (0 – 180°)
Mean direction, 50 – 75% lines	**Low (0 – 30°)**	**Medium – High (bimodal, significant peak 95 – 175°, 2nd smaller peak 30 – 80°)**	Medium – High (wide, 70 – 180°, bimodal)	Low – High (0 – 180°)
Total length, all lines	**Low < 5000 m**	Low (2500 – 3500 m)	Low– High (trimodal, 5000 – 22500 m)	Low – High (2500 – 25000 m)
Data	**Storø group**	**Bjørneøen group**	**Isua group**	**Background**